

Groundwater temperature anomalies in the vicinity of salt domes in central Poland show potential for low-temperature geothermal energy

Patryk BLADUSIAK^{1, 2, *}, Tomasz OPERACZ¹ and Kamil PAWELEC¹

- ¹ Polish Geological Institute – National Research Institute, Carpathian Branch in Krakow, Skrzatów 1, 31-560 Kraków, Poland; ORCID: 0009-0000-7622-8341 [P.B.], 0000-0003-4950-1933 [T.O.], 0000-0003-2475-6470 [K.P.]
- ² AGH University of Krakow, Al. Adama Mickiewicza 30, 30-059 Kraków, Poland



Bladusiak, P., Operacz, T., Pawelec, K., 2026. Groundwater temperature anomalies in the vicinity of salt domes in central Poland show potential for low-temperature geothermal energy. *Geological Quarterly*, **70**, 12; <https://doi.org/10.7306/gq.1857>

Associate Editor: Beata Jaworska-Szulc

One of the few examples of renewable energy sources independent of weather conditions is geothermal energy, utilized both in high-temperature geothermal systems and, increasingly, in low-temperature geothermal applications. We describe novel research on the influence of salt diapir structures on groundwater temperatures in their surroundings. The Łanięta and Lubień salt domes in Poland were selected as representative study areas. Based on a series of field studies, temperature distribution maps were developed for Quaternary, Neogene, and Paleogene aquifers. The analysis demonstrated that groundwater thermal anomalies in the vicinity of salt diapirs reach up to +2.0°C. The results obtained enabled an assessment of the potential for utilizing this additional thermal energy in low-temperature geothermal systems. A temperature anomaly in the range of +0.5 to +2.0°C translates directly into a measurable improvement in system coefficients of performance, thereby reducing operational costs. The course of action proposed in this paper for identifying optimal locations for shallow geothermal energy exploitation has not been previously applied and represents an effective approach to maximizing the share of renewable energy sources and enhancing the diversification of local energy supplies, particularly in central and eastern Europe, where salt dome geological structures are relatively common.

Key words: salt dome, geothermal heat, thermal anomalies, groundwater, low-temperature geothermal energy.

INTRODUCTION

Salt domes are common in many sedimentary basins worldwide. In Europe, they are among the most numerous groups of structures within sedimentary basins. The oldest such basins in the world are Precambrian in age, while the youngest are Cenozoic (Belenitskaya, 2018). Within such basins, complex salt structures develop, such as salt pillows, salt ridges and diapirs (Poborska-Młynarska, 2022).

Halokinetic movements within Zechstein (Upper Permian) salt strata lead to significant and complex transformations in Mesozoic and Cenozoic structures (Górski and Rasala, 2009). These processes continue to operate in some regions, and the resulting deformations have a significant impact on the local geological environment (Daniilidis and Herber, 2017). The rate of halokinesis may exceed 19 mm/year; its course is continuous

and can be observed using remote sensing methods (Piątkowska et al., 2012).

Salt structures also significantly influence groundwater flow and transport, influencing the coupling between hydraulic forces and the geothermal gradient (Teixeira et al., 2014). Temperature distribution depends primarily on the configuration of Zechstein salts and factors such as salt thickness and salt table depth (Ondrak et al., 1998; Scheck-Wenderoth et al., 2014). The thermal conductivity (K) of salt is up to three times higher than that of the surrounding strata (Vizgirda et al., 1985; Blackwell and Steele, 1989; Mello et al., 1995; Grunnaleite and Mosbron, 2019; Degen et al., 2022; Raymond et al., 2022).

These properties of salt in salt formations can be utilized to generate renewable energy from geothermal heat in both shallow and deep geothermal systems. Low-temperature geothermal energy, also referred to as shallow or low-enthalpy geothermal energy, is thermal energy of both endogeneous and exogeneous origin that is extracted from the uppermost part of the lithosphere, typically at depths of ~200–400 m (Klonowski et al., 2020). This conventionally adopted depth limit varies considerably depending on local and regional natural conditions, legal regulations, scientific approaches, and applied technologies. In Europe, the temperature of the shallow subsurface layer is variable and influenced by factors such as ambient atmospheric air

* Corresponding author, e-mail: pblad@pgi.gov.pl

Received: January 27, 2026; accepted: March 20, 2026; first published online: May 5, 2026

temperature. However, it tends to stabilize at depths of ~15–20 m, and below this level it is partly controlled by the local geothermal gradient. As a result, the temperature of the shallow ground layer – forming a low-temperature geothermal system – can be continuously harnessed throughout the year using ground-coupled heat pump installations (Self et al., 2013; Sarbu and Sebarchievici, 2014; Casasso et al., 2017). Deep geothermal energy, on the other hand, refers to the use of thermal energy stored in deep layers of the Earth's crust, typically at depths exceeding 1 km, where natural reservoirs of elevated-temperature geothermal waters occur. This energy is accessed through geothermal drilling, which allows for the extraction of hot water or steam from deep aquifers and their use primarily in heating systems and, under favourable conditions, for electricity production. In Poland, deep geothermal resources are primarily associated with the sedimentary basins of the Polish Lowlands and the Podhale region, where favourable geological and hydrothermal conditions exist for the exploitation of geothermal waters (Górecki et al., 2006; Kępińska et al., 2015).

Previous modelling of salt structures from various regions of the world has provided valuable information on their impact on ambient thermal conditions (Yu et al., 1992; Petersen and Lerche, 1995). However, studies of the impact of salt structures

have focused primarily on depths exceeding 100 m and on levels older than the Cenozoic (Scheck-Wenderoth et al., 2014; Negulic and Loudon, 2017). Examples include the Hydra and Sørvestlandet salt domes located east of the Central Ridge on the southwestern part of the Norwegian North Sea shelf (Fig. 1; Grunnaleite and Mosbron, 2019). These studies have shown that, due to the high thermal conductivity of salt, the temperature in the area of the dome roots decreases by ~20°C, while in their upper parts, the rock temperature increases. This leads to the formation of thermal anomalies in the rocks above the domes, which can reach values as high as 8.5°C (Agemar et al., 2012; Grunnaleite and Mosbron, 2019).

In the New Orleans region, numerical modelling has been used to describe the impact of the West Bay salt dome on the temperature distribution in its surroundings (Fig. 1). The presence of salt domes was found to be the primary factor generating thermal anomalies, and there is no basis for assuming alternative mechanisms for their formation. Temperature anomalies were recorded along the entire borehole profile, reaching a maximum of ~25°C at a depth of 3,000 m (Vizgirda et al., 1985).

In Poland, ground investigations were conducted to determine the low-temperature geothermal potential within the Góra salt dome (Fig. 1). Surface geothermal measurements con-

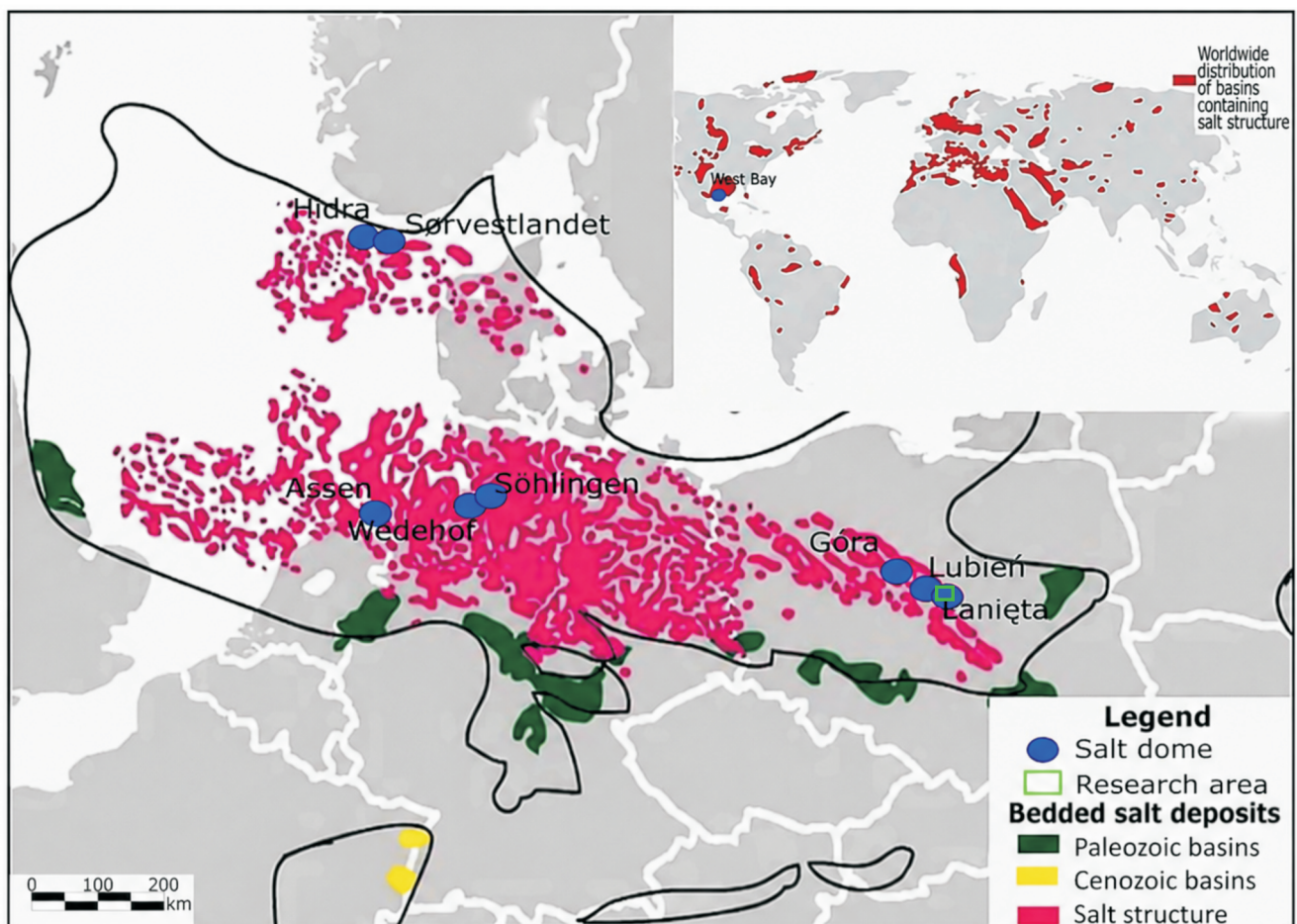


Fig. 1. Location of selected salt structures (after Hudec and Jackson, 2007; Donadei and Schneider, 2016; Krzywiec et al., 2017; Caglayan et al., 2020; Martin-Clave et al., 2021, modified)

firmed that the Góra salt dome is an area where the temperature measured above the dome is higher than its surroundings. The amplitudes of the recorded temperatures in the profiles analysed reached values of up to 1.4°C. The characteristic zonation in the temperature distribution, observed along profiles transverse to the dome, corresponded to the differential thermal conductivity of the rocks that make up both the dome itself and its surroundings (Tarkowski et al., 2003).

Groundwater occurring in the vicinity of salt domes is also an important aspect. Groundwater can play a significant role in shaping the temperature distribution, as shown, for instance, by studies conducted in the Gorleben dome area (Fromme et al., 2010). The likelihood of groundwater influencing temperature increases with decreasing rock cover thickness (Jensen, 1983). In saturated zones where intense groundwater flow is observed, heat transport from salt columns or domes occurs much faster than in regions with limited groundwater flow (Fromme et al., 2010). The small thickness of the strata in the Wedehof and Söhlingen (Fig. 1) salt domes, composed of highly permeable Quaternary deposits, indicates a high probability of groundwater impacting the local temperature field (Fromme et al., 2010). Variations in the thermal conductivity of the overlying rock layers cause local temperature fluctuations at the top of the salt dome. These differences remain small, yet they result in significant temperature anomalies in its upper reaches. Studies of the thermal conditions of salt dome structures and the assessment of their practical implementation as geothermal heat sources have been a recognized research direction in Poland for at least two decades (Petersen and Lerche, 1995). Previous projects focused on the use of thermal water resources, proposing the exploitation of waters with temperatures of up to 100°C from Mesozoic and Paleozoic levels located up to several kilometres below ground level (Górecki et al., 2006; Szewczyk and Gientka, 2009). In deep geothermal boreholes, an effect of temperature (so-called thermal lift) is observed, which results in the volumetric expansion of the fluid extracted (Operacz et al., 2020). For the region covered by the research in this study, only temperature values on general maps of Poland have been shown so far for a depth of 0.5 m b.g.l., and these amounted to 9.0°C (Górecki et al., 2006).

Temperature studies in shallow aquifers near Assen (Fig. 1) have shown that water temperature increases in areas with salt domes range from 0.3 to 1.0°C (Janssen, 2015). The temperature difference between aquifers in areas without salt domes and those in areas affected by salt domes in a steady-state model was ~2.5°C. This temperature difference occurred at depths of up to 120 m (Janssen, 2015).

In this context, our work is innovative in seeking to demonstrate that the same geophysical mechanism (the so-called “thermal chimney” – Petersen and Lerche, 1995; Pająk, 2005) also generates shallow anomalies (at depths <100 m). Our research empirically indicates that the occurrence of thermal anomalies in groundwater at shallow depths can be of significant economic importance for commonly used, low-temperature ground-source heat pump systems.

The results of previously published studies indicate the potential of utilizing energy from such positive temperature anomalies in groundwater around salt domes. However, testing this hypothesis requires detailed recognition and analysis of local conditions. This work presents the results of innovative re-

search on the impact of the Łanięta and Lubień salt domes (Fig. 1) on hydrogeothermal conditions and the mechanism of temperature anomalies in their vicinity.

STUDY AREA

GEOLOGICAL CHARACTERISTIC

The Łanięta and Lubień salt domes, encompassing parts of the Kuyavian-Pomeranian and Łódź voivodeships, were selected as the reference study area (Fig. 2). This is an area where optimal use of low-temperature geothermal energy can significantly improve the balance of renewable energy sources. Other renewable sources, such as flowing water, wind, or solar energy, are relatively rarely used due to unfavourable natural conditions. Furthermore, their use is often hampered by potential social protests and changing legal constraints (Operacz and Tomaszewska, 2016). Therefore, it is highly desirable to explore areas and opportunities for using other, even low-temperature, sources, such as those described in this article. The structure analysed is typical of salt domes, and therefore the research results obtained are relevant to other geologically similar areas.

The study region is located in north-central Poland, within the Polish Lowlands. The crystalline basement of the region consists of Precambrian-Paleozoic platform units, while Paleozoic-Mesozoic sedimentation was associated with the evolution of the Permian-Mesozoic basin. The platform cover is covered by sedimentary strata deposited continuously since the Paleozoic, with Carboniferous and Permian rocks occurring locally, which are closely related to the development of the Permian Basin in central Europe.

Within the study area, a number of salt structures occur, including many domes and pillows, which are manifestations of halokinetic reorganization of Zechstein salts. Recognized salt structures in this region include the Lubień and Łanięta domes (Fig. 2). The Łanięta and Lubień salt structures studied are located in the eastern part of the European Permian Basin (Peryt et al., 2010; Krzywiec et al., 2017 with references therein). The Permian stratigraphic sequence is represented here mainly by the Rotliegend red shales and sandstones overlain by Zechstein cyclothems (Upper Permian), dominated by carbonates, anhydrites, and thick rock salt beds (Peryt and Kiersnowski, 2026). Geophysical studies and structural cross-sections have documented the diverse geometric forms of the Lubień and Łanięta domes – from nearly concentric salt domes to extensive pillows – which reflect the variable dynamics of halokinetic processes and the significant influence of the overburden architecture on the direction of their development, to create the present-day structures. The domes are likely rooted in the same Wojszyce salt dome, and thus have a similar internal geological structure (Krzywiec, 2004; Czapowski and Tarkowski, 2018).

The salt structure of the Łanięta dome comprises a complete sequence of Zechstein evaporites representing cyclothems PZ2, PZ3 and PZ4. Their thickness varies considerably due to intense diapiric deformation (Czapowski and Tarkowski, 2018; Czapowski et al., 2025; Fig. 3).

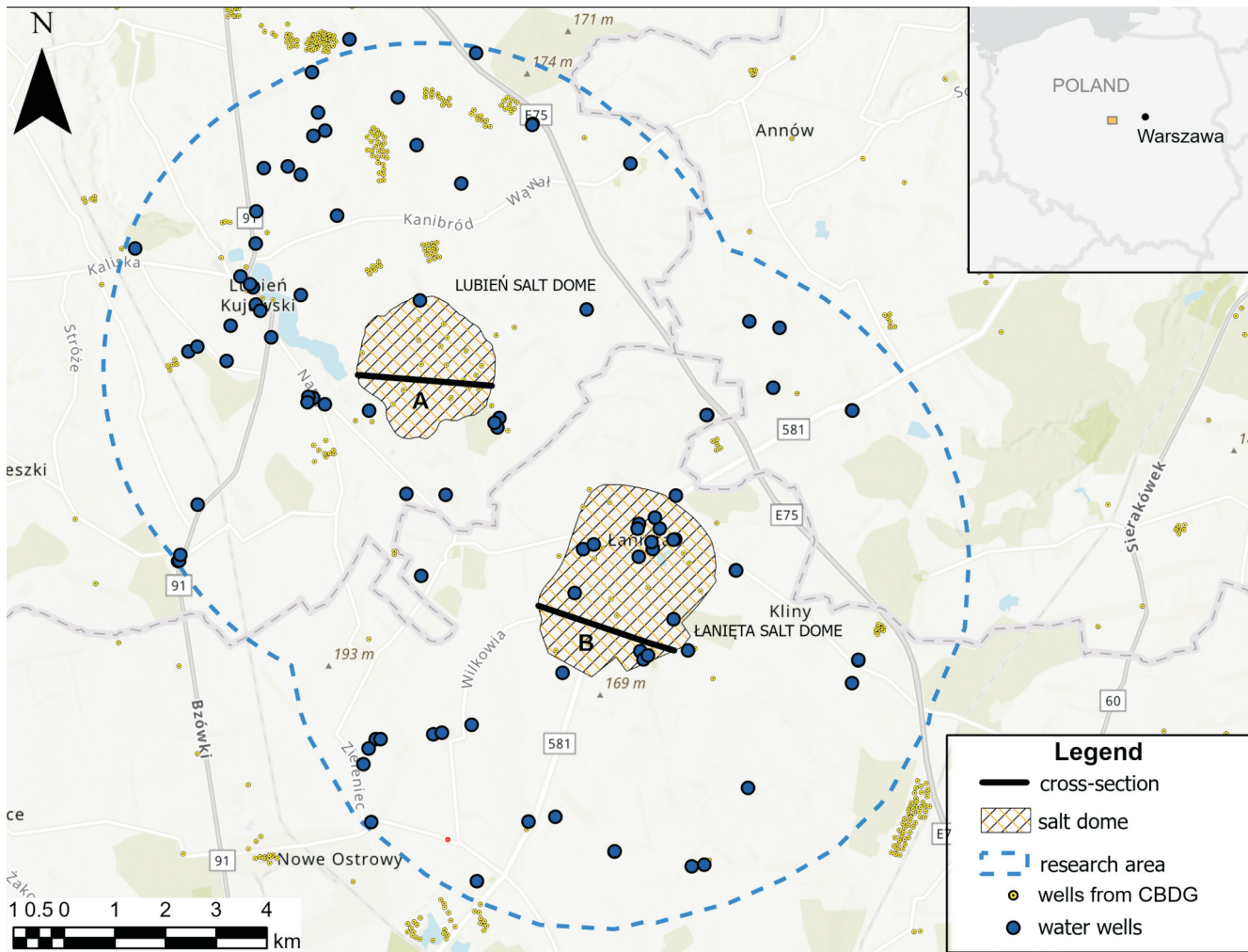


Fig. 2. Study area of the Łanięta and Lubień salt domes

Cross-sections A and B are shown in [Figure 3](#)

The PZ2 cyclothem is represented by the Basal Anhydrite A2 (up to ~104 m), overlain by the Older Rock Salt Na2 reaching ~257 m and locally accompanied by the Older Potassium Salt K2 (~7 m).

The PZ3 cyclothem consists of the Brown Zuber Na3t (~104 m), Younger Rock Salt Na3 (~86 m) and Main Anhydrite A3 (~120 m).

The PZ4 cyclothem includes the Youngest Rock Salt Na4 (~41 m) and the Red Zuber Na4t, which locally exceeds 100 m in thickness ([Chelmiński et al., 2016](#)).

The evaporite sequence is overlain by a gypsum-anhydrite-clay cap with a thickness ranging from ~29 to 241 m, formed as a result of dissolution, redeposition and chemical transformation processes affecting the upper part of the diapir ([Chelmiński et al., 2016](#); [Czapowski and Tarkowski, 2018](#)).

The Lubień dome is also composed of Zechstein evaporites of cyclothem PZ2, PZ3 and PZ4, and its internal structure reflects multi-stage diapiric deformation and intense mobility of plastic salt masses during diapir intrusion ([Czapowski and Tarkowski, 2018](#); [Fig. 3](#)).

Within the PZ4 cyclothem, Red Zuber Na4t reaches up to 95.6 m in thickness, while Youngest Rock Salt Na4 attains up to 61.4 m.

The PZ3 cyclothem is dominated by the Younger Rock Salt Na3 with a maximum thickness of 254.1 m. The Main Anhydrite A3, locally interbedded with the Platy Dolomite Ca3 and the Grey Salt Clay T3, reaches up to 78.7 m.

The PZ2 cyclothem includes the Older Rock Salt Na2 with a thickness of up to 359.4 m, accompanied by the Older Potassium Salt K2 (up to 6.7 m). These deposits overlie the Anhydrite A2r (~10.2 m) and Basal Anhydrite A2, which together reach 103.4 m and occur in 10–15 layers ([Czapowski and Tarkowski, 2018](#)). As indicated by [Trusheim \(1957\)](#), the development of pillows, diapirs and salt columns requires the presence of salt deposits exceeding 300 m in thickness and an overburden of at least 1000 m thick ([Chelmiński et al., 2016](#)). The area analysed is located in the middle zone of the salt tectonics, where salt structures, such as dykes, columns, and diapirs, were most fully developed, partially or completely penetrating Mesozoic rocks ([Dadlez, 1997](#); [Fig. 3](#)).

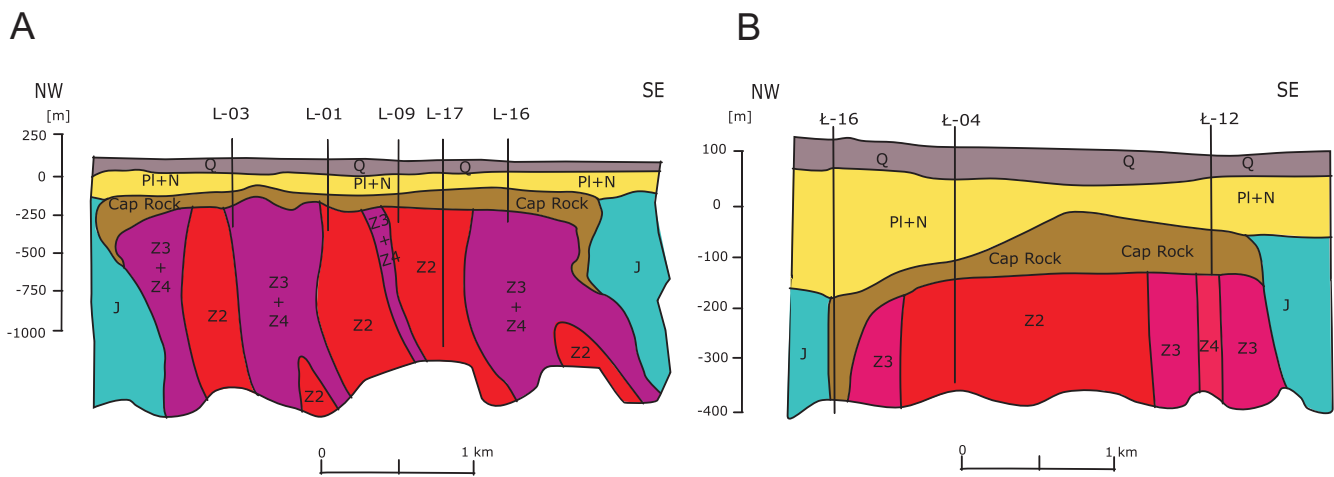


Fig. 3. Cross-sections through the Lubień and Łanięta salt domes

A – simplified cross-section through the Lubień salt dome (after K. Poborska-Młynarska in: Ślizowski et al., 2004);

B – simplified cross-section through the Łanięta salt dome (after Parecka, 1980, modified);

location of cross-sections is shown in Figure 4

In vertical section, Mesozoic, Paleogene and Neogene rocks occur above the Zechstein formations, while the ground surface is composed of Quaternary deposits, which locally mask the structural expression of the salt domes and determine contemporary geomorphological processes (Fig. 3). The Quaternary deposits in the area are characterized by significant variability in thickness, from several tens of metres in the central part of the Łanięta salt dome to ten or so metres on the periphery. They are dominated by river sands and gravels up to 3.5 m thick, accumulated as terraces of the Wisła River valley.

The Paleogene and Neogene deposits are represented by the Poznań variegated clays and Miocene succession with interbedded lignite and silty sands. The oldest Neogene deposits – Miocene, Oligocene, and Pliocene – occur as clayey and sandy sequences with lignite interbeds, locally exceeding several tens of metres in thickness (Baraniecka, 1993; Roman, 2011).

The Pleistocene deposits, up to 40 m thick, are of diverse glacial and fluvio-glacial origin. They are represented by boulder clays, sands and gravels associated with the Central Polish Glaciation (Krzywiec, 2009). Holocene deposits in the northern part of the study area consist primarily of fluvial and dune sands, colluvial clays, peats and alluvial soils.

HYDROGEOLOGICAL CONDITIONS

The study area is located within the administrative boundaries covered by four hydrogeological map sheets: Lubień Kujawski, Gostynin, Krośniewice and Kutno. The local hydrogeological system is multi-layered and was analysed based on the detailed hydrogeological maps of the Main Usable Aquifer (GUPW) and the First Groundwater Horizon (PPW).

The GUPW is predominantly associated with Quaternary fluvio-glacial and fluvial sands and gravels, and locally with Neogene sands (Oficjańska and Krawczyńska, 2002; Włostowski

and Gregosiewicz, 2002a; Włostowski, 2002). These Quaternary aquifers occur at varying depths, typically down to 50 m, with the thickness of water-bearing strata generally ranging from 10 to 20 m. They are commonly separated by low-permeability glacial tills, while the deeper Neogene aquifers are isolated from the surface by thick layers of Pliocene Poznań variegated clays (Mikołajczyk, 2008; Sobolewska et al., 2012; Węgrzyn et al., 2012). Additionally, the southern part of the study area lies within the extent of the Major Groundwater Basin No. 226 (GZWP 226 Krośniewice-Kutno), a deep fractured-karstic reservoir developed in Upper Jurassic formations (Włostowski, 2002).

The Łanięta and Lubień salt domes significantly disrupt this regional hydrostratigraphy. Halokinetic movements and the piercing of salt diapirs through Mesozoic and Cenozoic strata create zones of tectonic loosening, faulting, and variable overburden thickness (Czapowski and Tarkowski, 2018). These structural disturbances establish direct vertical hydraulic pathways, facilitating contact between deeper, highly mineralized waters and the shallow aquifers (Baraniecka, 1993; Czapowski and Tarkowski, 2018).

Field measurements conducted in 20 observation wells (filtration depths 27–93 m b.g.l.) reflect these local hydrochemical interactions. The background shallow groundwater exhibits normal electrical conductivity (EC) mostly in the range of 240–600 $\mu\text{S}/\text{cm}$ and an alkaline character ($\text{pH} > 9.0$). However, near the salt structures, anomalous zones were identified where EC reaches up to 1084 $\mu\text{S}/\text{cm}$, accompanied by a slightly alkaline pH (7.3–8.0). The geological setting strongly supports the hypothesis of localized upward migration of brines along the fault zones surrounding the salt domes.

From a geothermal perspective, the high hydraulic conductivity of the Quaternary sands plays a crucial role (Węgrzyn et al., 2012; Hajdas and Woźniak, 2018). In these permeable horizons, advection becomes a dominant heat transport mechanism. The flowing groundwater effectively absorbs thermal en-

ergy from the underlying, highly conductive salt columns and distributes it laterally. This continuous advective heat transport significantly amplifies the local geothermal potential, contributing directly to the thermal anomalies observed in the shallow aquifers.

MATERIALS AND METHODS

FIELDWORK METHODOLOGY

Research on the impact of salt thermal conductivity was conducted in the Lubień and Łanięta salt domes, based on published literature from various regions of Europe, where similar structures caused thermal anomalies (Grunnaleite and Mosbronn, 2019).

Based on data from the Polish Geological Institute – National Research Institute Midas database (link: MIDAS), the extent of the Łanięta and Lubień salt domes was determined. A 5 km radius buffer was then established around their boundaries,

constituting the study area (Fig. 4). Fifty five groundwater intake boreholes exceeding 30 m in depth were identified within this designated area. Shallower boreholes were excluded from the study, recognizing that the temperature of the water drawn from them may be influenced by atmospheric or anthropogenic conditions. Detailed information about the boreholes was obtained from the HYDRO Bank (link: <https://spd.pgi.gov.pl/map>).

A *Solinst Levelogger 5* (for temperature profiling) and a compensating *Barologger 5* (Model 3001) were used for field studies. The *Levelogger 5* performed water temperature profiling with an accuracy of $\pm 0.05^\circ\text{C}$. pH and EC were measured using a Slandi pH metre and conductivity metre, respectively. *Levelogger* studies were conducted using the device's application which allows for a delay in the start of measurements (a 5 minute delay was set). After this delay, the actual measurement began. The purpose of the delay was to allow the sensor to thermally stabilize after immersion in water, so that its temperature could equalize with the water temperature before the actual recording began.

The measurements were divided into two groups: continuous measurements and point measurements. The locations of

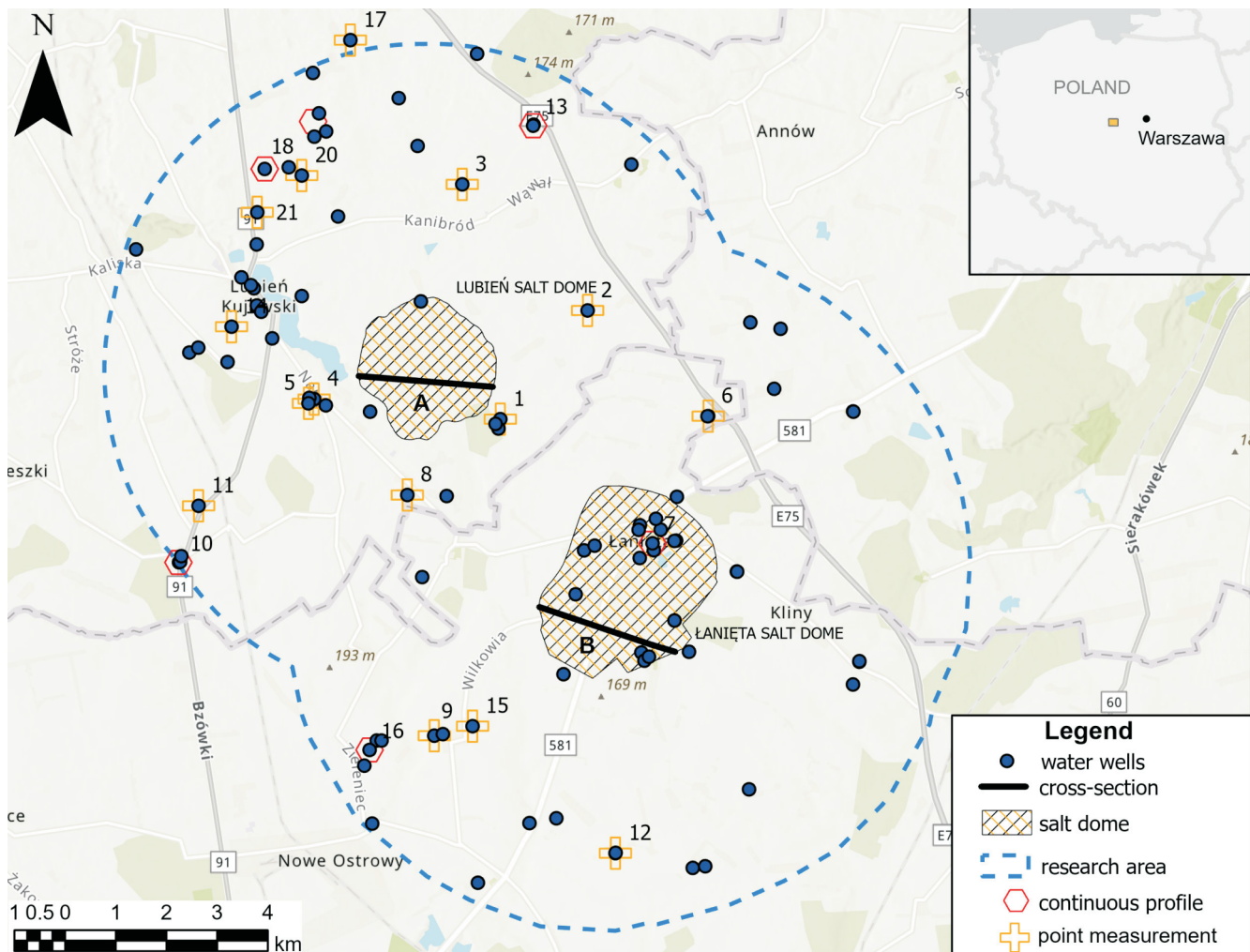


Fig. 4. Location of continuous and point temperature measurements

Well numbers in Table 1

the test points are shown in Figure 4. Continuous measurements consisted of creating a water temperature profile from the water table to the bottom of the well (as a temperature-depth profile). These were performed exclusively in unequipped boreholes (i.e., without water extraction installations). During these measurements, the apparatus was lowered at a rate of ~1 metre per 40 seconds (~0.025 m/s), and the recorder took measurements every 5 seconds. Point measurements were performed in “reinforced” boreholes. These involved collecting a water sample from the filtered level and simultaneously measuring its temperature.

Raw tabulated data (primarily from continuous profiling) enabled the creation of temperature-depth graphs and were used for further analysis in *Petrel 2020* (Schlumberger). The results of the point measurements may have been subject to error, as pump activation could have affected the water temperature. Therefore, in this study, they only served as supporting information for the continuous profiles.

Additionally, a control area was established, encompassing five boreholes located outside the zone of influence of the salt domes, yet drilled in formations with stratigraphy and lithology similar to those in the study area. This procedure enabled the

determination of a reference level (Fig. 5). Data from the TP-1 Halinów borehole, where the Polish Geological Institute – National Research Institute (PGI-NRI) conducts continuous temperature measurements, were also included in the analysis (Kłonowski and Żeruć, 2024). This borehole is located in rocks with lithology and stratigraphy comparable to both the control and study areas, and is also located outside the range of influence of the salt domes (Fig. 5).

To assess the potential impact of salt domes on water hydrochemistry, physicochemical parameters of the water were analysed: specific electrolytic conductivity (SEC) and pH. SEC is a measure of the water’s ability to conduct electricity and is directly related to total dissolved solids (TDS). In the context of research conducted near salt domes, SEC is a key, rapid proxy for identifying potential salinity zones, but also an indicator of potential anthropogenic contamination.

The research was conducted in two rounds: the first in late January and early February 2025, and the second in late June and early July 2025 (Fig. 6). The results confirmed the initial assumption that the season has no effect on groundwater temperature <30 m b.g.l., as the temperature difference was within the measurement error of the equipment. Furthermore, the field

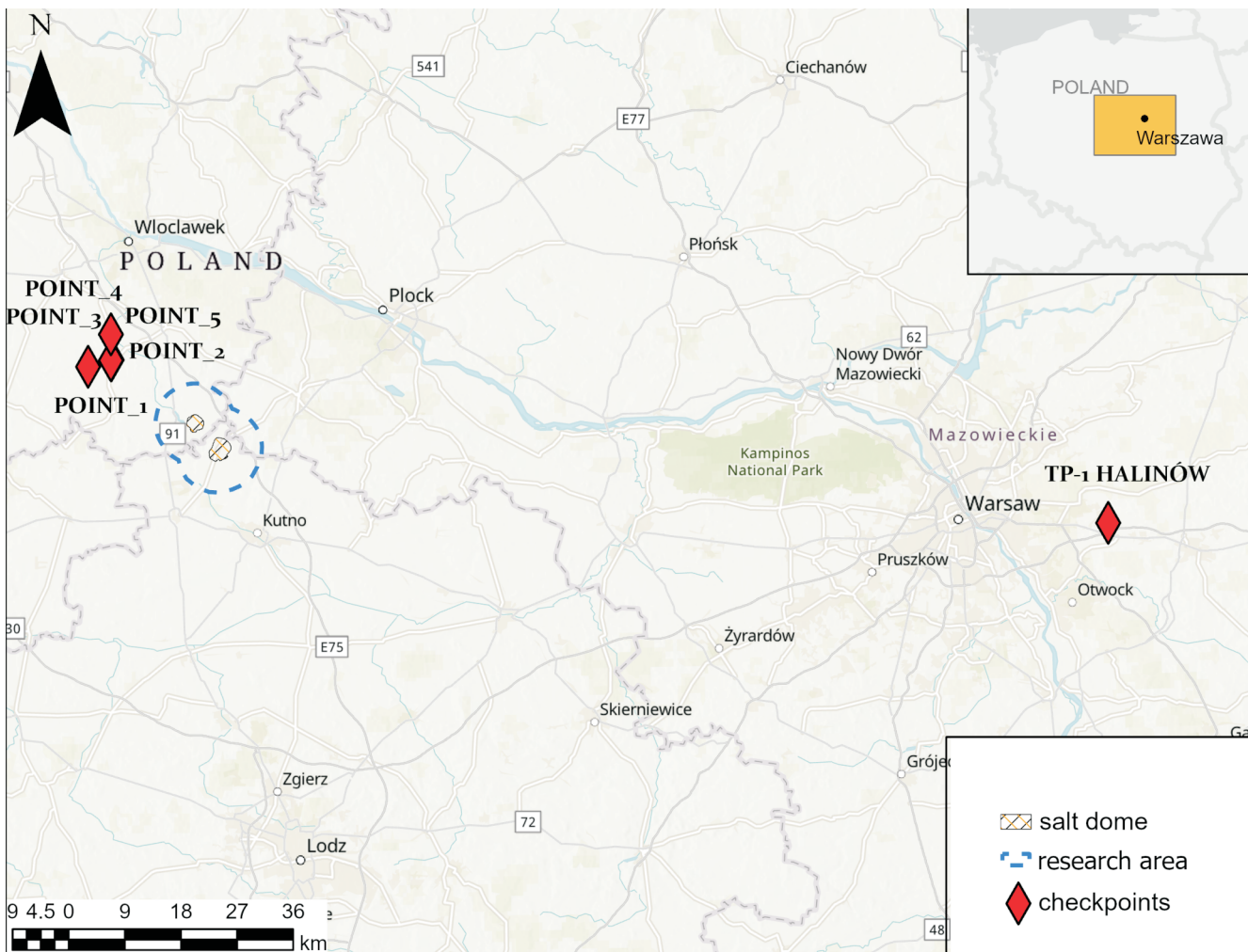


Fig. 5. Control area with the TP-1 Halinów test well

Table 1

List of research wells with physical parameters measured at the level of filtration

| No | Name of the well | Water temperature [°C] | EC [$\mu\text{S}/\text{cm}$] | pH | Filter depth from-to [m b.g.l.] | Notes |
|----|--|------------------------|--------------------------------|------|---------------------------------|---|
| 1 | 4800036 – "HYDROKOP" S2 | 10.265 | 394 | 7.78 | 42.1–50.0 | |
| 2 | 4810156 – PUNKT CZERPALNY ST 1 | 10.067 | 1084 | 7.3 | 39.7–45.7 | high EC |
| 3 | 4800061 – STUDNIA PUBLICZNA 1 | 9.813 | 671 | 7.52 | 33.2–39.2 | |
| 4 | 4800079 – WODOCIĄG WIEJSKI 2 | 9.997 | 447 | 7.38 | 33.8–43.8 | |
| 5 | 4800064 – WODOCIĄG WIEJSKI 3 | 10.001 | 242 | 6.82 | 37.9–41.3 | |
| 6 | 4810183 – WODOCIĄG WIEJSKI ST2 | 10.193 | 581 | 7.42 | 30.5–42.5 | |
| 7 | 4810055 – GORZELNIA 2 | ~11 | 794 | 8.06 | 78.0–93.0 | continuous temperature profile, high EC |
| 8 | 4800120 – GOSPODARSTWO ROLNE 1 | 10.19 | 428 | 7.4 | 68.0–86.0 | |
| 9 | 5160156 – WODOCIĄG WIEJSKI I SKR 2 | 10.019 | 541 | 7.43 | 42.9–57.1 | |
| 10 | 4800054 – ZAKŁAD ROLNY 3 | ~9.7 | 452 | 7.67 | 50.8–65.0 | continuous temperature profile |
| 11 | 4800089 – GOSPODARSTWO ROLNE 1 | 11 | 484 | 7.27 | 72.0–88.5 | |
| 12 | 5170119 – DOM POMOCY SPOŁECZNEJ 1 | – | 519 | 8.76 | 36.5–47.0 | |
| 13 | 4800188_PGR_ST_1 | ~9.3 | 275 | 9.07 | 54.5–58.5 | continuous temperature profile |
| 14 | 4800218 – POLCALC SP. Z O.O. 2 | – | 397 | 8.33 | 27.15–44.85 | |
| 15 | 5160188 – DESZCZOWNIA PLANTACJI OWOCÓW-1A | 10.6 | 383 | 8.43 | 31.0–36.0 | |
| 16 | 5160081 – ZAKŁADY PASZOWE 2 | ~10.4 | 245 | 9.48 | 39.5–49.5 | continuous temperature profile |
| 17 | 4800209 – GOSPODARSTWO ROLNE 1 | – | 628 | 8.31 | 38.0–47.0 | |
| 18 | 4800214 – GOSPODARSTWO ROLNE 1 | ~10.5 | 760 | 8.47 | 32.0–44.0 | continuous temperature profile high EC |
| 19 | 4800081 – GOSPODARSTWO ROLNE 2 | ~9.4 | 513 | 8.26 | 32.0–46.0 | continuous temperature profile |
| 20 | 4800059 – PUNKT CZERPALNY (D. UJĘCIE WIEJ) | – | 590 | 8.07 | 38.0–44.0 | |
| 21 | 4800200 – GOSPODARSTWO ROLNE 1 | – | 573 | 8.1 | 35.0–41.0 | |

studies provided information indicating no visible seasonal effect even from 20 m b.g.l. It was therefore possible to carry out research at different times of the year, because the research problem concerned waters below the level of influence of external factors such as air temperature.

METHODOLOGY OF ANALYTICAL WORK

Maps and models are used to identify potential geothermal deposits and thermal anomalies (Li et al., 2018). *Schlumberger's Petrel 2020* software was used to develop stratigraphic level maps and temperature maps. Archival data were used to create accurate three-dimensional maps of the area: maps, cross-sections, and well data on the stratigraphy of the wells. Data from 556 wells were prepared and organized, including by standardizing the stratigraphy using *Microsoft Excel*. Due to the lack of available digital information, it was necessary to create this. For this purpose, graphical maps previously imported into

Petrel software were digitized. Digitizing the maps allowed for the creation of isolines and the assignment of depths to them. Based on the isolines, maps were created using the Make Surface tool using the convergent interpolation algorithm and matching to the wells (with appropriate stratigraphic separation using the well adjustment option). A 50 x 50 m grid was used. This algorithm is often available for creating geological unit surfaces within structural or layered modelling. The algorithm was used to obtain top stratigraphic surfaces based on point data while reproducing the morphological trends of a given surface as accurately as possible and avoiding excessive fluctuations (Sbrana et al., 2018). As part of this study, it was decided to create maps of three stratigraphic levels: the Holocene at a depth of 20 m b.g.l. (Fig. 7), the Pleistocene, which was combined with the Holocene at a depth of 20 m b.g.l. (Fig. 8), and a Paleogene-Neogene map (Fig. 9). The decision to prepare a Holocene map for a depth of 20 m b.g.l. was dictated by the fact that a temperature anomaly map was developed for this depth. The analysis of fieldwork results described in this article confirms



Fig. 6. Field research in the area of Lubień and Łanięta salt domes

A – well 5160081 – ZAKŁADY PASZOWE 2; B – well 4800079 – WODOCIĄG WIEJSKI 2;
 C, D – well 4810055 – GORZELNIA 2; location of wells on [Figure 4](#)

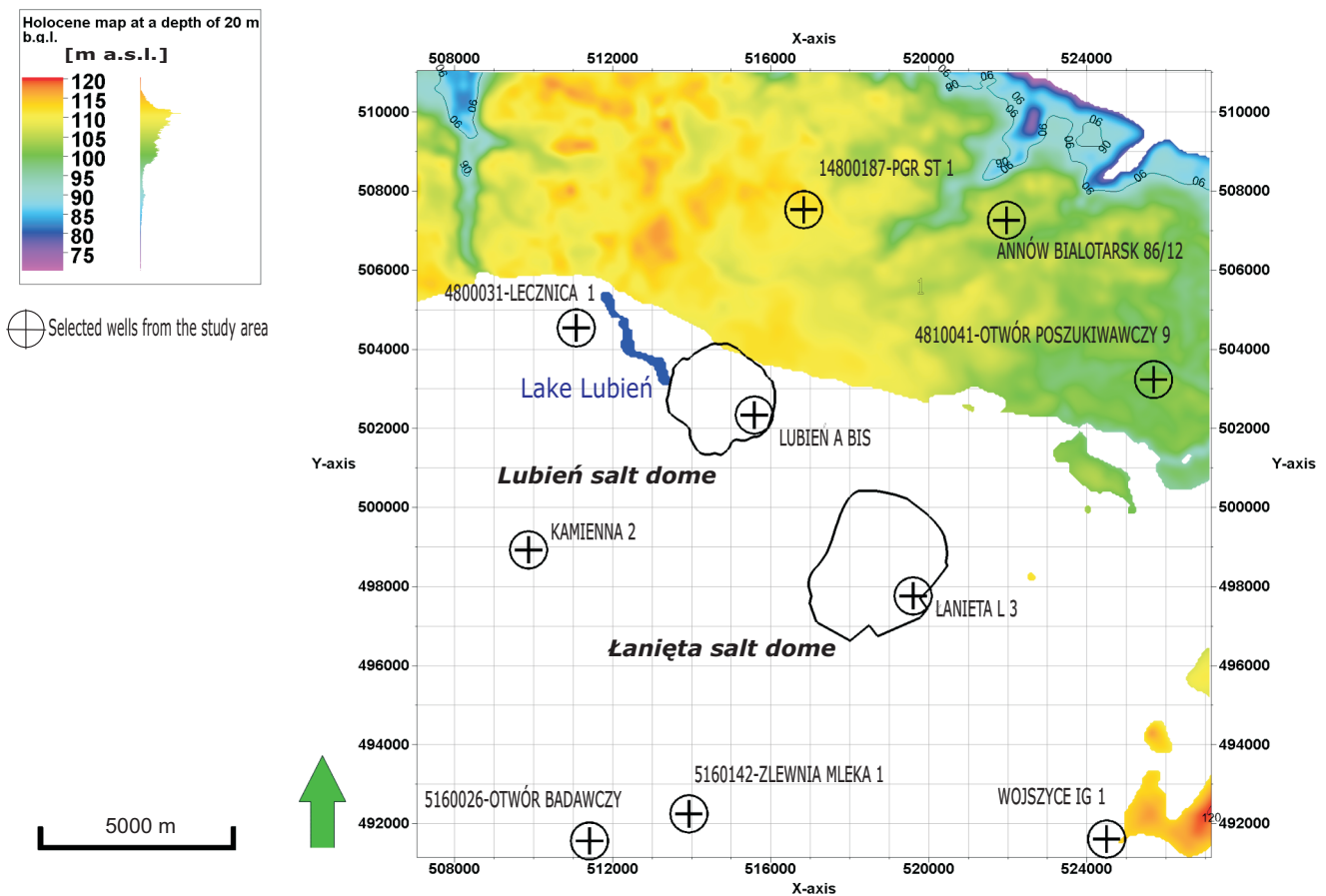


Fig. 7. Holocene map at a depth of 20 m b.g.l.

that, even below a depth of 20 m, there is no observed effect of surface meteorological conditions on rock temperature. Subsequent map levels were prepared for the tops of stratigraphic units. Based on the structural maps and temperature data obtained from the fieldwork, temperature maps were prepared. The primary research material consisted of continuous temperature profiles obtained in seven “unreinforced” wells. Supplementary data included results from ten active boreholes where point measurements were taken, as well as information from the TP-1 Halinów well and the control area (Kłonowski and Żeruń, 2024).

RESULTS AND DISCUSSION

As a result of field studies conducted in accordance with the methodology described above, a database of temperature, EC and pH was obtained for 20 study sites in the vicinity of the Łanięta and Lubień salt domes, shown in Figure 4. The results obtained are summarized in Table 2.

EC values for the groundwater tested in the 20 wells show significant variability, ranging from 242 to 1084 $\mu\text{S}/\text{cm}$ (Table 1). Most samples (~75% of the tested wells) fall within the 240–600 $\mu\text{S}/\text{cm}$ range. This range can be considered the local hydro-

chemical background for shallow Quaternary and Paleogene-Neogene waters, representing typical normal groundwater.

Three wells clearly stand out from the dominant groundwater. These are boreholes with numbers 4810156 (EC = 1084 $\mu\text{S}/\text{cm}$), 4810055 (EC = 794 $\mu\text{S}/\text{cm}$) and 4800214 (EC = 760 $\mu\text{S}/\text{cm}$).

Such high EC values in shallow aquifers, in the immediate vicinity of the Łanięta and Lubień salt domes, strongly suggest a local inflow of highly mineralized waters. Although brine migration from deeper levels might be a natural hypothesis in the context of the salt domes, these values (in the range of 760–1084 $\mu\text{S}/\text{cm}$) are also typical of anthropogenic contamination, for example, of agricultural origin (fertilizers) or municipal origin (leaky septic tanks). Considering the shallow location of the studied waters and the agricultural nature of many wells, the latter hypothesis seems more likely.

Analysis of the hydrochemical data also revealed an interesting relationship between pH and EC. Waters with the lowest mineralization (EC < 300 $\mu\text{S}/\text{cm}$) were observed to exhibit an alkaline pH (pH > 9.0). Anomalous waters, identified as potential contamination zones (EC > 750 $\mu\text{S}/\text{cm}$), were characterized by a slightly alkaline pH (pH 7.3–8.06). This inverse correlation may indicate the mixing of two genetically distinct water types: shallow, alkaline freshwater, evolving in Quaternary deposits,

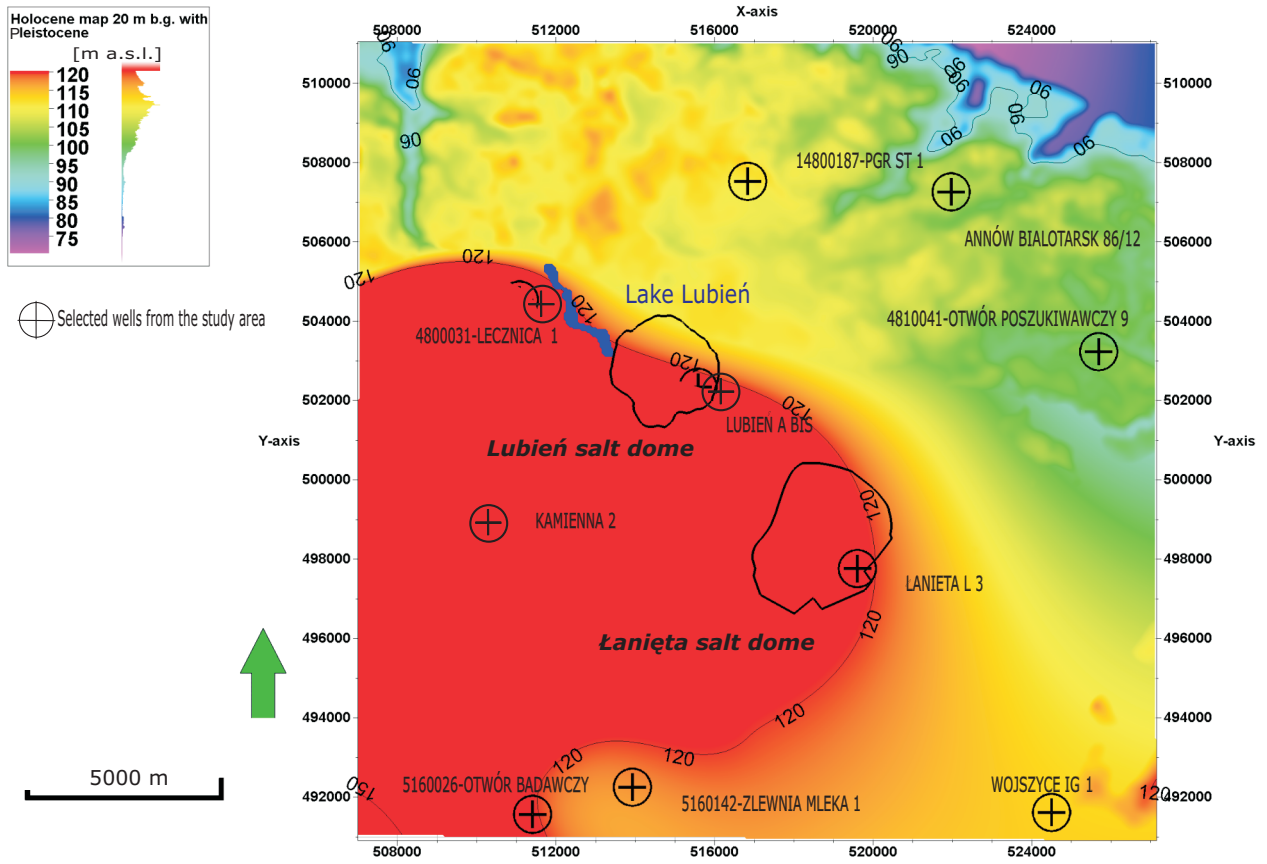


Fig. 8. Map of the Holocene top with the Pleistocene at a depth of 20 m b.g.l.

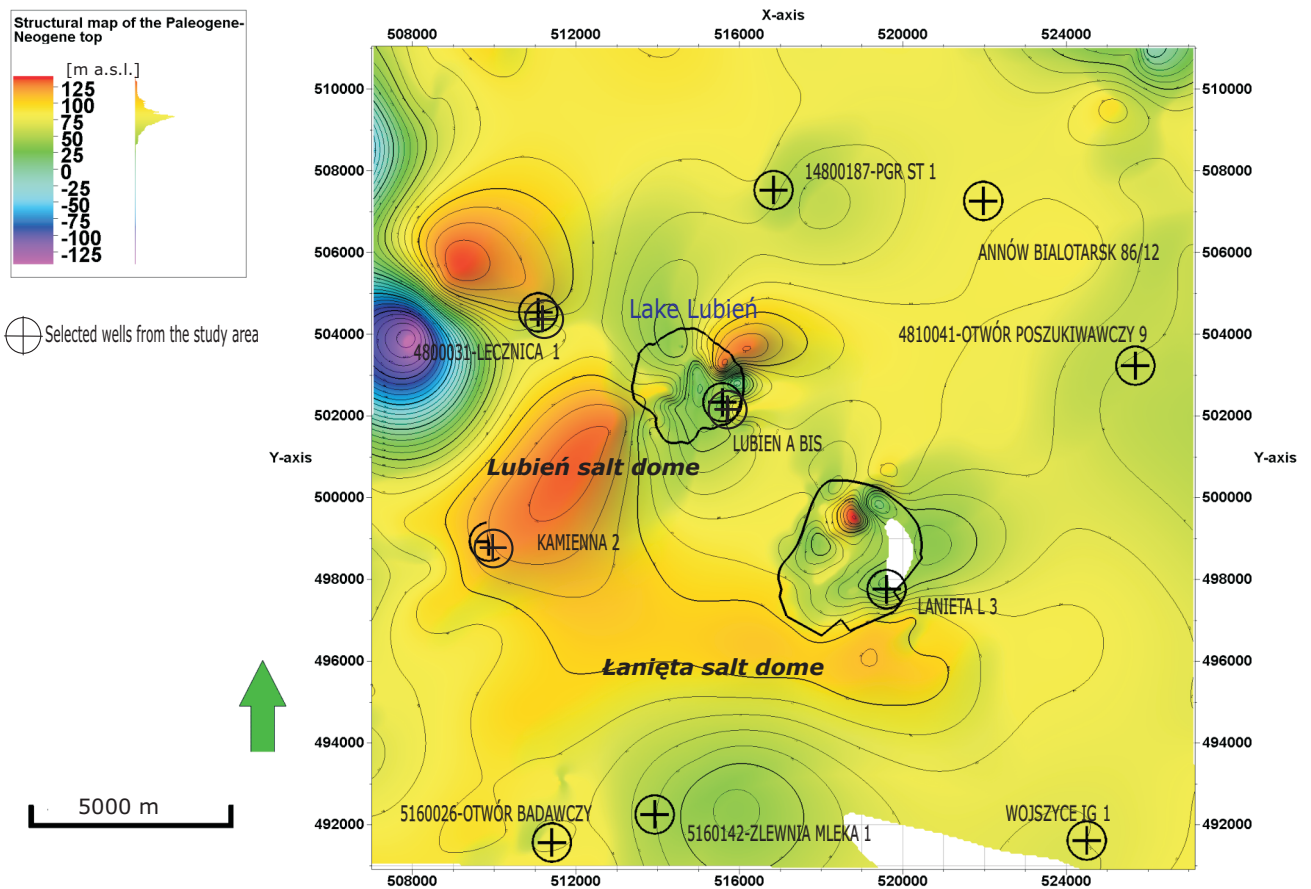


Fig. 9. Structural map of the Paleogene-Neogene top

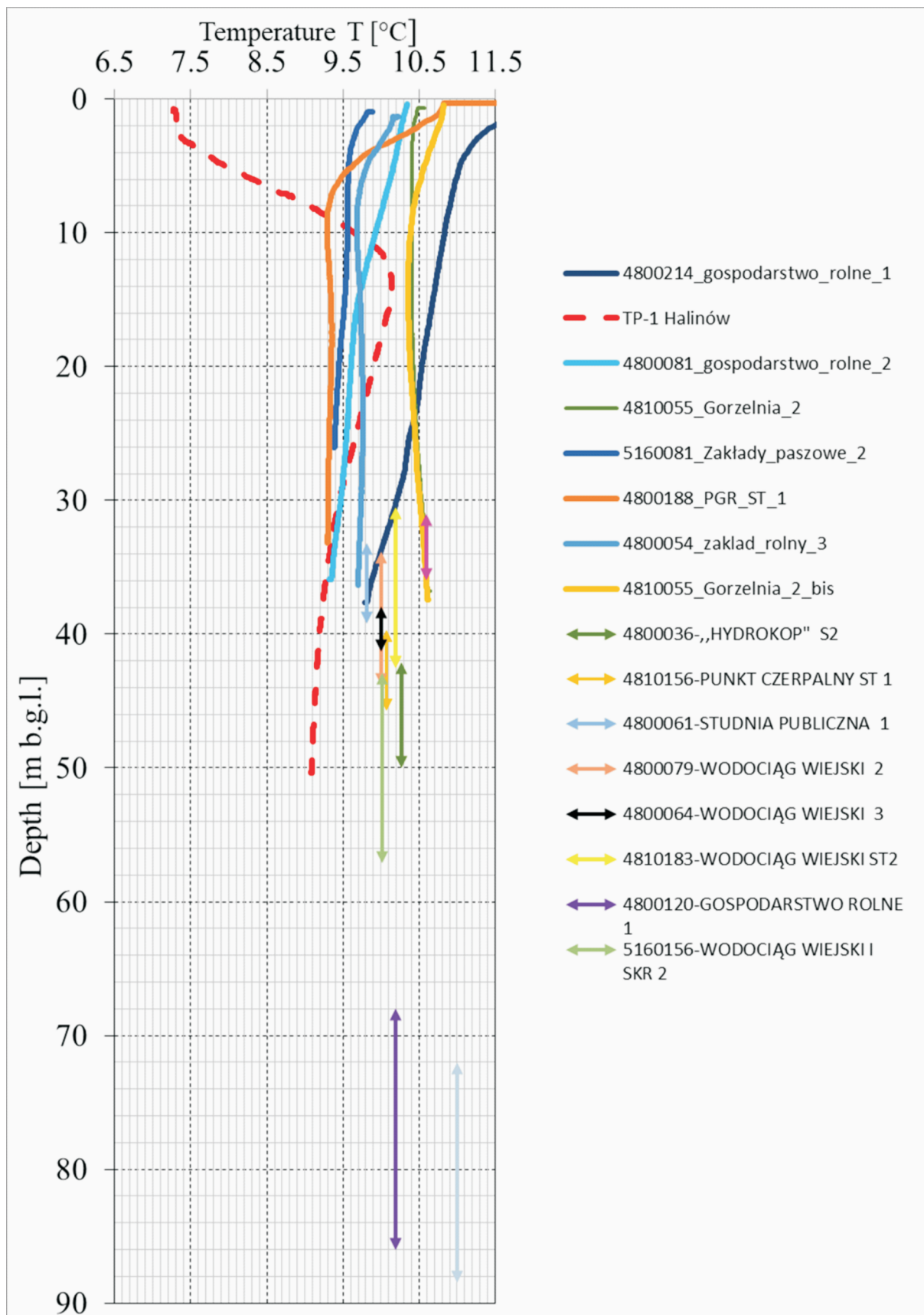


Fig. 10. Summary of “continuous” and “point” measurements with control areas

Table 2

Temperature difference between the ground and the working medium

| Thermal anomaly [°C] | Water temperature in rocks/soil [°C] | ΔT (soil-medium) [°C] |
|----------------------|--------------------------------------|-------------------------------|
| 0°C (baseline) | 9 | $9 - 2 = 7$ |
| +0.5 | 9.5 | $9.5 - 2 = 7.5$ |
| +1 | 10 | $10 - 2 = 8$ |
| +2 | 11 | $11 - 2 = 9$ |

and a component derived from pollution (e.g., agricultural or municipal), which is more hydrochemically neutral. The inflow of this latter component increases mineralization (EC) but simultaneously lowers the pH of the mixture, acting as a buffer for the alkaline waters of the shallow aquifers.

It was decided to describe the temperature at stratigraphic horizons (Figs. 8 and 9) and compare the temperature profiles with the lithological profiles of wells where continuous measurements were possible (Fig. 10). Based on the results obtained, a field data summary was prepared, comparing the temperature profiles from the study area with the temperature profile from the TP-1 Halinów well (Fig. 10). The TP-1 Halinów well is derived from archived data from the PGI-NRI (Klonowski and Żeruń, 2024) and represents the temperature background used as a reference point for identifying and interpreting temperature anomalies. The continuous profiles are treated as reference data because they are not distorted by external influences, such as well pump operation, which can affect the results of point measurements. Additionally, a summary was prepared, correlating the data from the TP-1 Halinów well and the control area with the results obtained from both continuous profiles and point measurements (Fig. 10). Continuous measurements were also used later in the study to prepare temperature distribution maps.

In the study area, water temperatures in wells at depths of >20 b.g.l. ranged from 9.5 to 11.0°C (Fig. 10), and the background temperature ranged from 9.0 to 9.7°C (Fig. 10). Anomalous values were observed around the Łanięta and Lubień salt domes. The reduced temperature values around the dome (considered anomalous) may be related to disturbances caused by the impact of a natural lake, Lake Lubień, the impact of which can lower water temperatures in aquifers. Shallow water bodies, such as Lake Lubień, have enormous heat capacity and are strongly linked to atmospheric conditions. They act as seasonal thermal buffers. Shallow groundwater in the immediate vicinity of the lake is in constant thermal interaction with the lake water. As a result, the temperature of these waters is a result of atmospheric conditions, not a deeper geothermal flow. The lake therefore acts as a local buffer that effectively eliminates the positive anomaly resulting from the salt domes.

A lack of visible external influence on temperature was also observed from a depth of ~20 m b.g.l. This indicates that the initial assumption of temperature constancy from 30 m b.g.l., based on published data, was overstated. This also leads to the

conclusion that the temperature anomalies observed resulted from the impact of heat from salt domes.

The temperature distribution in the study area was analysed for individual stratigraphic units – from Holocene deposits at a depth of 20 m b.g.l. to Paleogene-Neogene formations.

In the Holocene-Pleistocene deposits at a depth of 20 m b.g.l., temperature values range from 9.3 to 10.5°C (Fig. 11). Elevated temperatures are visible around the salt domes, particularly in their northern parts, where the salt table with a gypsum cap is closest to the ground surface (Fig. 11). In the Paleogene-Neogene strata, groundwater temperatures range from 9.5 to 11°C (Fig. 12). The highest groundwater temperatures were also observed in these strata near the Lubień and Łanięta salt domes (Fig. 14). This phenomenon is related to the effective heat transport by salt, which conducts thermal energy from deeper geological layers. No impact related to the lake’s presence was observed in the unit analysed.

The thermal anomalies detected demonstrate a significant impact on the increase in the geothermal potential of the study area. Temperature anomalies reaching up to +2.0°C were identified in the study area (Figs. 11 and 12).

The lithology of the rocks surrounding the salt dome also has a significant impact on heat transport, and thus on temperature increases. Stratigraphy and lithology are based on the HYDRO Bank database. Lithological observations require a deeper interpretation of heat transport mechanisms (Figs. 13–15). In low-temperature geothermal energy, two processes must be distinguished: conduction, i.e., heat transport through static material, dominant in low-permeability deposits (such as boulder clays), and advection (convection), i.e., heat transport through the movement of a carrier (groundwater), dominant in high-permeability lithologies (sands, gravels) (Busby et al., 2009). In the context of ground-source heat pumps, groundwater flow is very beneficial because it causes continuous thermal “regeneration” of the ground around the heat exchanger, preventing it from cooling excessively during the heating season. It can be hypothesized that the observed strong anomalies (up to +2°C) are the result of a combined effect: high conduction through the salt dome, which transports heat from the depths of the Earth, and high advection in the Quaternary aquifers (sands/gravels), where the groundwater effectively “receives” this heat from the dome and distributes it to the measurement wells (Figs. 13–15).

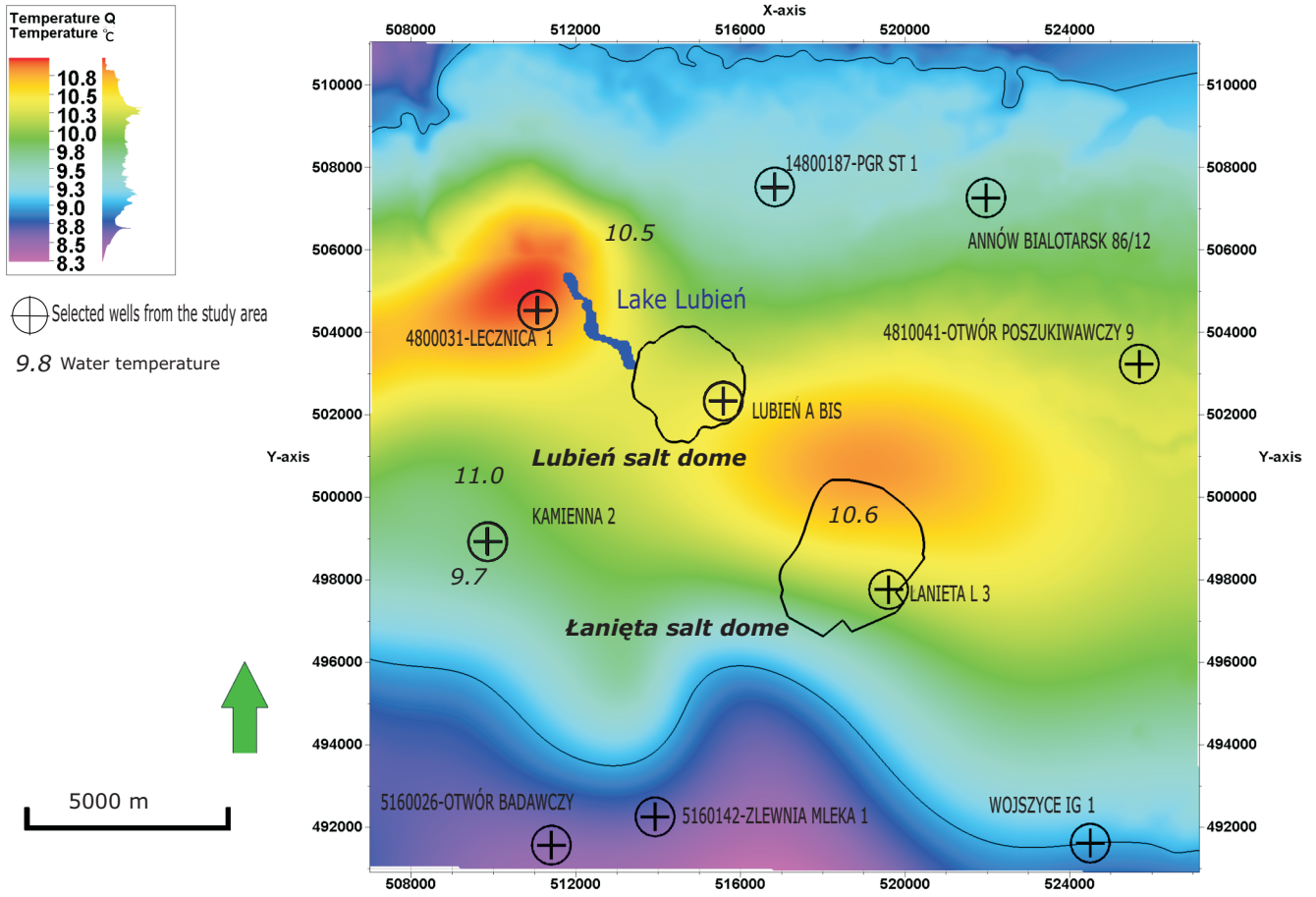


Fig. 11. Map of the Holocene top with the Pleistocene at a depth of 20 m b.g.l.

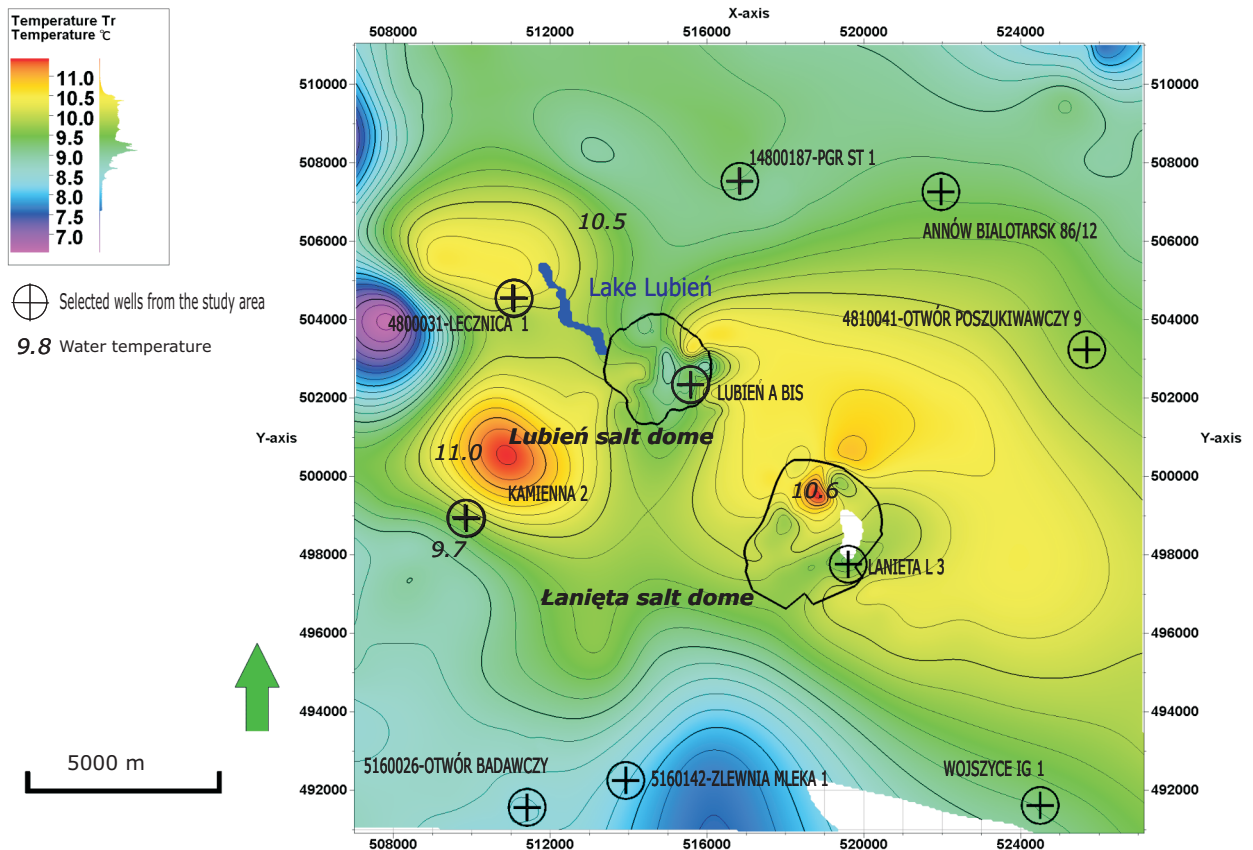
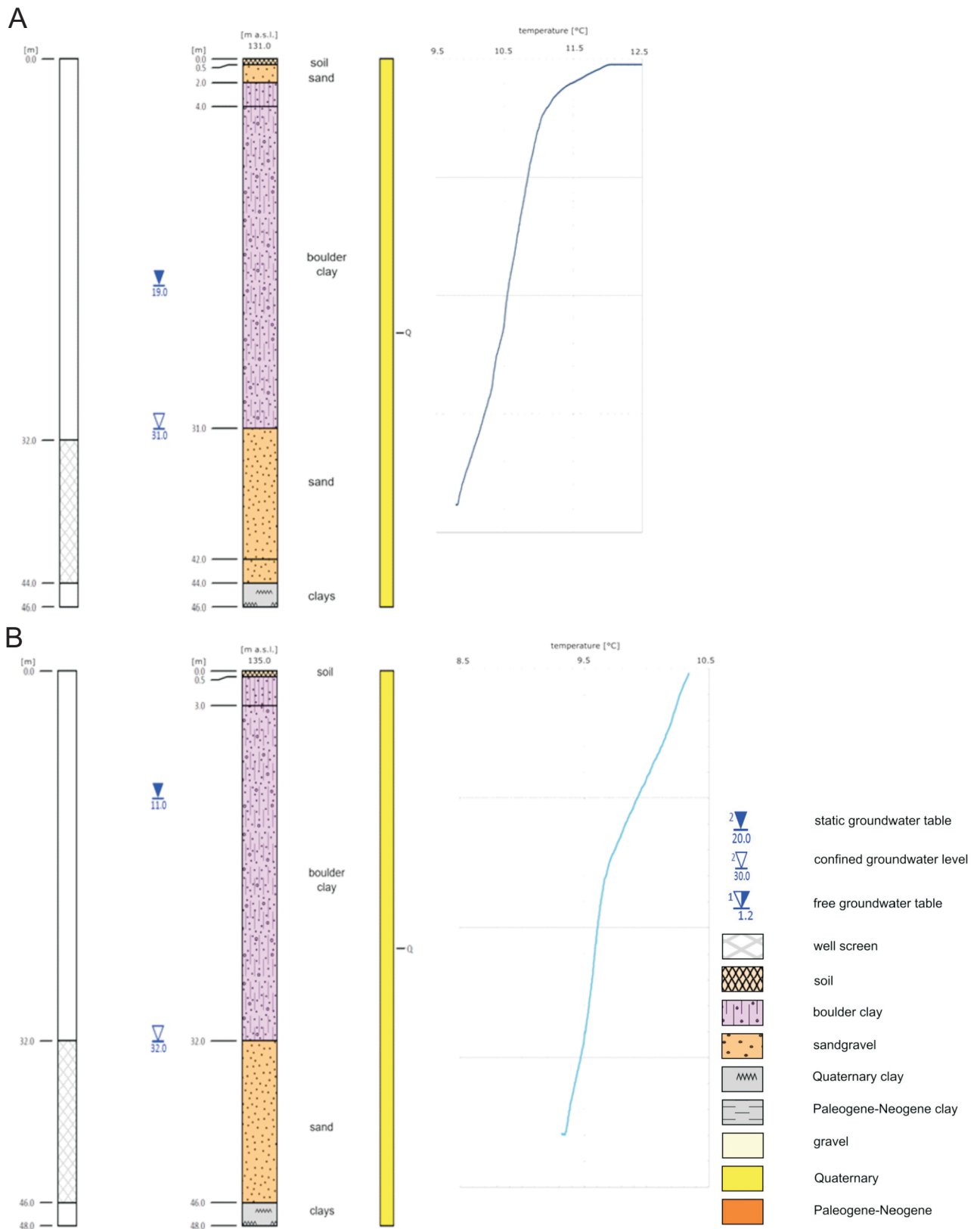


Fig. 12. Groundwater temperature distribution map for the Paleogene-Neogene top



**Fig. 13A – well 4800214 – Gospodarstwo rolne 1 with temperature profile;
B – well 4800081 – Gospodarstwo rolne 1 with temperature profile**

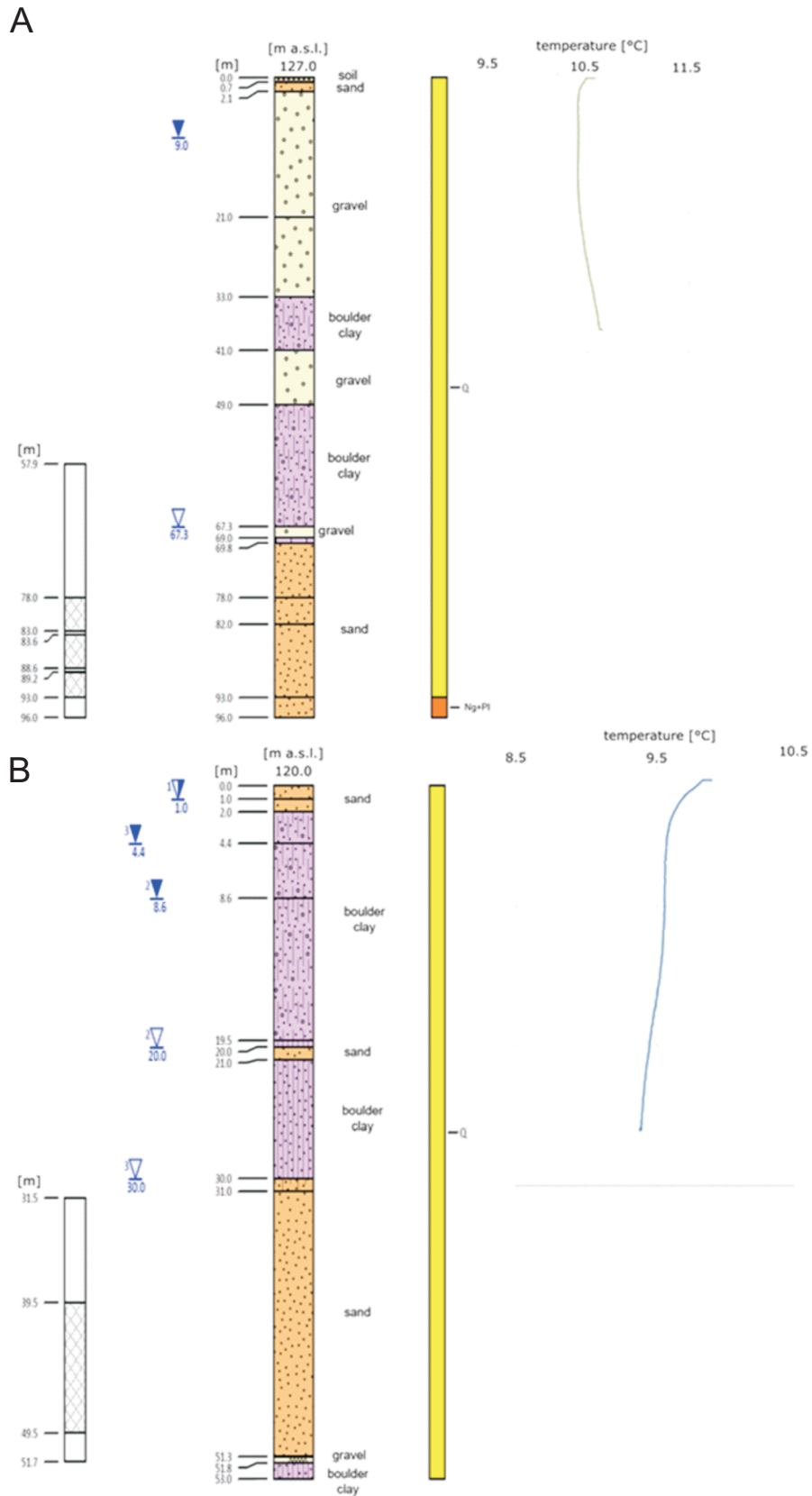


Fig. 14A – well 4810055 – Gorzelnia 2 with temperature profile;
 B – well 5160081 – Zakłady Paszowe 2 with temperature profile

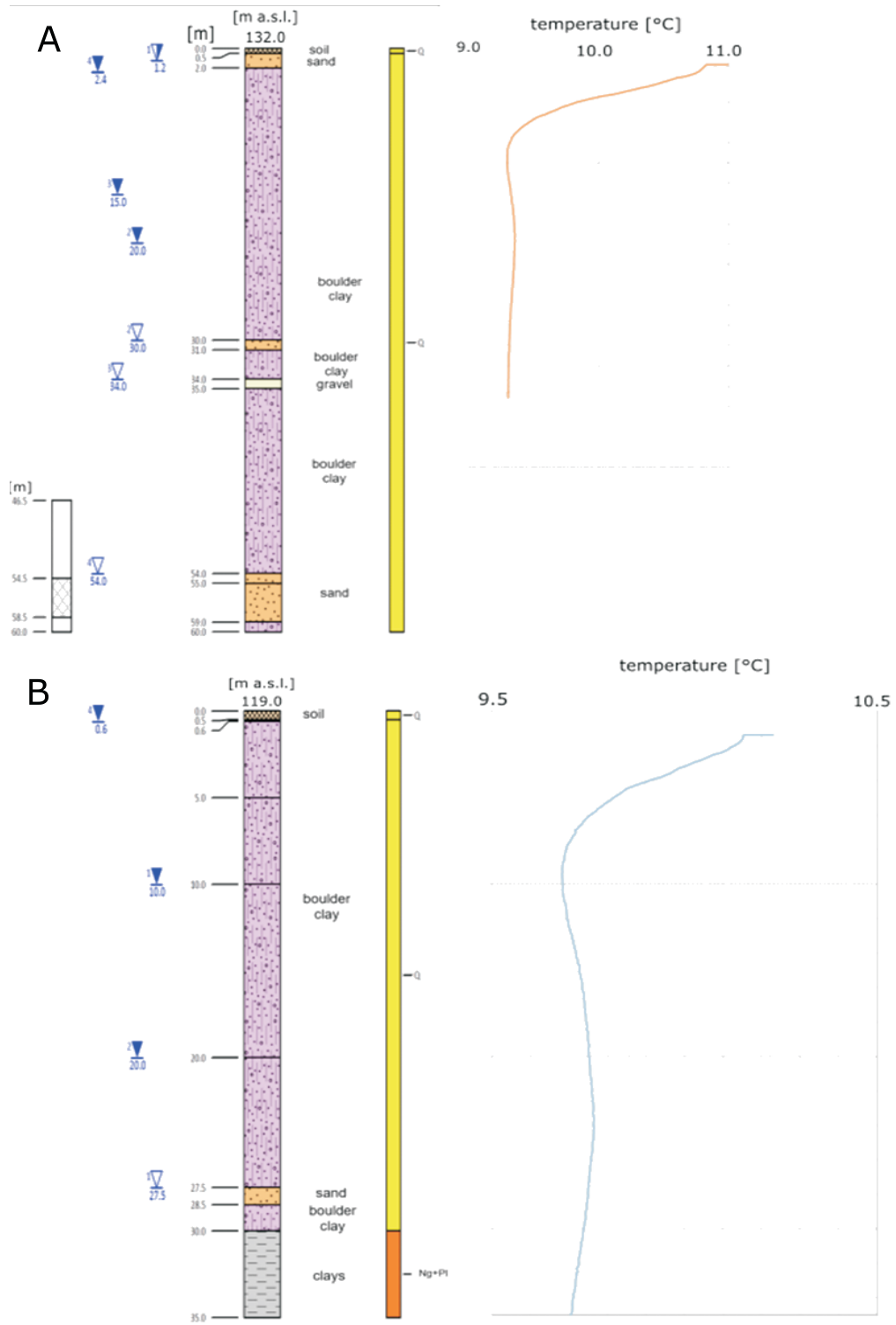


Fig. 15A – well 4800188 – PGR ST 1 with temperature profile;
 B – well 4800054 – Zakład rolny 3 with temperature profile

To estimate the scale of the increased thermal impact of the salt domes, a simplified model based on Fourier's law of thermal conductivity was used, enabling the assessment of relative (percentage) changes in thermal power.

The thermal power P is described by equation [1]:

$$P = k \times A \times \Delta T \quad [1]$$

where: P – thermal power (W); k – effective heat transfer coefficient ($\text{W}/\text{m}^2\text{K}$); A – heat transfer surface (m^2); ΔT – temperature difference between the ground and the working medium ($^{\circ}\text{C}$)

The following calculation assumptions were made for the analysis:

- the ground outlet temperature (T_g) is 9°C ;
- the working medium (e.g., the glycol solution in the ground-source heat pump system) has a temperature of 2°C ;
- the heat transfer coefficient k was assumed to be a constant value, as the purpose of the analysis was to determine relative changes, not absolute power values;
- the heat transfer surface A was assumed to be constant and not to affect the percentage change in geothermal potential.

Table 3 shows the temperature difference between the ground and the working medium for various thermal anomaly scenarios.

Table 3

Percentage change in geothermal potential depending on the size of the thermal anomaly

| Thermal anomaly [$^{\circ}\text{C}$] | ΔT [$^{\circ}\text{C}$] | Increased geothermal potential [%] |
|--|-----------------------------------|------------------------------------|
| 0 | 7 | 0 |
| +0.5 | 7.5 | 7.1 |
| +1 | 8 | 14.2 |
| +2 | 9 | 28.5 |

Taking into account that power is related to temperature difference, the potential increase in its value was approximated, expressed as a percentage. Formula [2] for the potential increase was used:

$$P = \frac{T}{T} - 1 \quad 100\% \quad [2]$$

where: ΔT – temperature difference between the ground and the working medium; T – ground temperature without the impact of the salt dome.

Based on calculations, it was found that due to the impact of the salt domes, the geothermal potential in this region can increase by up to 28.57%. Table 3 summarizes the potential changes for selected variants of water temperature increase in the region studied.

As a result of field studies and advanced analysis of the results obtained, it was found that the natural temperature increase observed in the vicinity of salt domes results in an increase in geothermal potential. A temperature increase of even 0.5°C results in a 7% increase in geothermal potential, while a 2°C increase (as observed in the study area) results in a 30% increase in potential. These are extremely significant values and represent significant value for the practical use of geothermal energy, particularly in low-temperature geothermal installations such as ground-source heat pumps.

CONCLUSIONS

Based on groundwater temperature studies conducted in the area of salt domes, it was empirically confirmed that the Łanięta and Lubień salt domes act as “thermal chimneys” generating measurable and stable positive temperature anomalies in shallow aquifers. From a depth of ~ 20 m b.g.l., there are no noticeable external factors disrupting the influence of the salt domes. It was demonstrated that the anomaly identified, of up to $+2.0^{\circ}\text{C}$, has a direct, positive economic impact on low-temperature geothermal energy and translates into increased efficiency of installations utilizing low-temperature geothermal potential. A systematic temperature increase was observed towards the salt structures, confirming their influence on the local thermal field. The only place where the impact of the salt dome is limited or completely eliminated is the area around the natural Lake Lubień. The temperature anomalies recorded, both above the salt domes and in the surrounding strata, can be used in the design of closed geothermal systems, increasing their profitability. The innovative research methodology developed has potential applications in the analysis of any salt structures with similar hydrogeological conditions worldwide, where groundwater occurs. Implementation is planned for other salt domes located in central Europe.

Acknowledgements. The authors would like to thank the editors and reviewers for constructive comments which helped to improve this manuscript.

REFERENCES

- Agemar, T., Schellschmidt, R., Schulz, R., 2012.** Subsurface temperature distribution in Germany. *Geothermics*, **44**: 65–77; <https://doi.org/10.1016/j.geothermics.2012.07.002>
- Baraniecka, M.D., 1993.** Objaśnienia do Szczegółowej mapy geologicznej Polski w skali 1:50 000, arkusz Lubień Kujawski (480) (in Polish). Państwowy Instytut Geologiczny, Warszawa.
- Belenitskaya, G., 2018.** Salt systems of the earth: distribution, tectonic and kinematic history, salt-naphthids interrelations, discharge foci, recycling. John Wiley & Sons, Hoboken; <https://doi.org/10.1002/9781119479208>
- Blackwell, D.D., Steele, J.L., 1989.** Thermal conductivity of sedimentary rocks: measurement and significance. In: *Thermal History of Sedimentary Basins: Methods and Case Histories* (eds. N. D. Naeser and T.H. McCulloh): 13–36. Springer, New York; https://doi.org/10.1007/978-1-4612-3492-0_2
- Busby, J., Lewis, M., Reeves, H., Lawley, R., 2009.** Initial geological considerations before installing ground source heat pump systems. *Quarterly Journal of Engineering Geology and Hydrogeology*, **42**: 295–306; <https://doi.org/10.1144/1470-9236/08-092>
- Caglayan, D.G., Weber, N., Heinrichs, H.U., Linßen, J., Robinus, M., Kukla, P.A., Stolten, D., 2020.** Technical potential of salt caverns for hydrogen storage in Europe. *International Journal of Hydrogen Energy*, **45**: 6793–6805; <https://doi.org/10.1016/j.ijhydene.2019.12.161>
- Casasso, A., Pestotnik, S., Rajver, D., Jez, J., Prestor, J., Sethi, R., 2017.** Assessment and mapping of the closed-loop shallow geothermal potential in Cerno (Slovenia). In: *European Geosciences Union General Assembly 2017. EGU Division Energy. Resources and Environment. ERE, Vienna*; <https://doi.org/10.1016/j.egypro.2017.08.210>
- Chelmiński, J., Czapowski, G., Małolepszy, Z., Nowacki, Ł., Rosowiecka, O., Stępień, U., 2016.** Integration of subsurface data for refinement of geological structure of salt diapirs; Łanięta salt diapir case (in Polish with English summary). *Salt Review*, **12**: 98–113.
- Czapowski, G., Tarkowski, R., 2018.** Geology of selected salt domes in Poland and their usefulness in constructing hydrogen storage caverns (in Polish with English summary). *Biuletyn Państwowego Instytutu Geologicznego*, **472**: 53–82; <https://doi.org/10.5604/01.3001.0012.6905>
- Czapowski, G., Bukowski, K., Razowska-Jaworek, L., Tomaszewska, B., Tyszer, M., Burliga, S., 2025.** Assessment of the possibility of obtaining selected critical elements (boron, magnesium, strontium) in Poland. *Przegląd Geologiczny*, **73**: 275–296; <https://doi.org/10.7306/2025.28>
- Dadlez, R., 1997.** Epicontinental basins in Poland: Devonian to Cretaceous – relationship between the crystalline basement and sedimentary infill. *Geological Quarterly*, **41**: 419–432.
- Daniilidis, A., Herber, R., 2017.** Salt intrusions providing a new geothermal exploration target for higher energy recovery at shallower depths. *Energy*, **118**: 658–670; <https://doi.org/10.1016/j.energy.2016.10.094>
- Degen, D., Veroy, K., Wellmann, F., 2022.** Uncertainty quantification for basin-scale geothermal conduction models. *Scientific Reports*, **12**, 4246.
- Donadei, S., Schneider, G.S., 2016.** Compressed air energy storage in underground formations. *Storing Energy*. In: *With Special Reference to Renewable Energy Sources* (ed. L.F. Cabeza): 113–133. Elsevier, Amsterdam; <https://doi.org/10.1016/B978-0-12-803440-8.00006-3>
- Fromme, K., Michalzik, D., Wirth, W., 2010.** Das geothermische Potenzial von Salzstrukturen in Norddeutschland. *Zeitschrift der Deutschen Gesellschaft für Geowissenschaften*, **161**: 323–333; <https://doi.org/10.1127/1860-1804/2010/0161-0323>
- Górecki, W. (ed.), Szczepański, A., Sadurski, A., Hajto, M., Papiernik, B., Kuźniak, T., Kozdra, T., Soboń, J., Szewczyk, J., Sokołowski, A., Strzetelski, W., Haładus, A., Kania, J., Kurzydłowski, K., Gonet, A., Capik, M., Śliwa, T., Ney, R., Kępińska, B., Bujakowski, W., Rajchel, L., Banaś, J., Solarzski, W., Mazurkiewicz, B., Pawlikowski, M., Nagy, S., Szamałek, K., Feldman-Olszewska, A., Wagner, R., Kozłowski, T., Malenta, Z., Sapińska-Śliwa, A., Sowizdzał, A., Kotyza, J., Leszczyński, K.P., Gancarz, M., 2006.** Atlas of Geothermal Resources of Mesozoic Formations in the Polish Lowlands. AGH University of Science and Technology, Kraków; Ministry of Environment; National Fund for Environmental Protection and Water Management, Warszawa.
- Górski, J., Rasala, M., 2009.** Hydrogeological conditions in salt dome areas and their significance for the safety of economic exploitation of salt structures (in Polish with English summary) *Biuletyn Państwowego Instytutu Geologicznego*, **436**: 121–128.
- Grunnalaite, I., Mosbron, A., 2019.** On the significance of salt modelling – example from modelling of salt tectonics, temperature and maturity around salt structures in southern North Sea. *Geosciences*, **9**, 363; <https://doi.org/10.3390/geosciences9090363>
- Hajdas, M., Woźniak, M., 2018.** Objaśnienia do Mapy hydrogeologicznej Polski w skali 1:50 000, arkusz Kutno (517) – Pierwszy Poziom Wodonośny (in Polish). Państwowy Instytut Geologiczny – PIB, Warszawa.
- Hudec, M.R., Jackson, M.P.A., 2007.** Terra infirma: understanding salt tectonics. *Earth-Science Reviews*, **82**: 1–28; <https://doi.org/10.1016/J.EARSCIREV.2007.01.001>
- Janssen, F.P.C., 2015.** Influence of the heat flow anomaly above a salt dome on shallow water temperature in the Drentsche Aa. Ph.D. Thesis, Faculty of Science and Engineering.
- Kępińska, B., Kasztelewicz, A., Pająk, L., Bujakowski, W., Tomaszewska, B., Hołojuch, G., 2015.** Introduction to geothermal energy, state and prospects of its development in the GEOCOM countries. In: *Handbook of best practices of geothermal resources management. PAS MEERI*: 9–18.
- Kłonowski, M.R., Żeruń, M., 2024.** Shallow subsurface temperature at the selected locations in Poland. *Proceedings of the 49th Workshop on Geothermal Reservoir Engineering*. Stanford University, Stanford, CA, USA, 12–14 February 2024.
- Kłonowski, M.R., Kocyła, J., Ryżyński, G., Żeruń, M., 2020.** Evaluation and statistical interpretation of low-temperature geothermal energy potential for selected locations in Poland. *Geological Quarterly*, **64**: 506–514; <https://doi.org/10.7306/GQ.1534>
- Krzywiec, P., 2004.** Triassic evolution of the Kłodawa salt structure: basement-controlled salt tectonics within the Mid-Polish Trough (central Poland). *Geological Quarterly*, **48**: 123–134; <https://qq.pgi.gov.pl/article/view/7338Li>
- Krzywiec, P., 2009.** Geometry and evolution of selected salt structures in the Polish Lowlands in the light of seismic data (in Polish with English summary). *Przegląd Geologiczny*, **57**: 812–818.

- Krzywiec, P., Peryt, T.M., Kiersnowski, H., Pomianowski, P., Czapowski, G., Kwolek, K., 2017.** Permo-Triassic evaporites of the Polish Basin and their bearing on the tectonic evolution and hydrocarbon system, an overview. In: Permo-Triassic Salt Provinces of Europe, North Africa and the Atlantic Margins (eds. J.I. Soto, J.F. Flinch and G. Tari): 243–261. Elsevier, Amsterdam; <https://doi.org/10.1016/B978-0-12-809417-4.00012-4>
- Li, J., Zhang, Q., Zhang, Y., 2018.** Entropy theory-integrated information model for the assessment of geothermal potential: a case study of Tengchong County, Southwest China. *Environmental Earth Sciences*, **77**, 98; <https://doi.org/10.1007/s12665-018-7225-9>
- Oficjalska, H., Krawczyńska, B., 2002.** Objasnienia do Mapy hydrogeologicznej Polski w skali 1:50 000, arkusz Lubień Kujawski (480) – Główny Użytkowy Poziom Wodonośny (in Polish). Państwowy Instytut Geologiczny, Warszawa.
- Ondrak, R., Wenderoth, F., Scheck, M., Bayer, U., 1998.** Integrated geothermal modeling on different scales in the northeast German basin. *Geologische Rundschau*, **87**: 32–42; <https://doi.org/10.1007/s005310050187>
- Operacz, A., Tomaszewska, B. 2016.** The review of Polish formal and legal aspects related to hydropower plants. *Environmental Science and Pollution Research*, **23**: 18953–18959; <https://doi.org/10.1007/s11356-016-7466-7>
- Operacz, A., Bielec, B., Tomaszewska, B., Kaczmarczyk, M., 2020.** Physicochemical composition variability and hydraulic conditions in a geothermal borehole – the latest study in Podhale Basin, Poland. *Energies*, **13**, 3882; <https://doi.org/10.3390/en13153882>
- Martin-Clave, C., Ougier-Simonin, A., Vandeginste, V., 2021.** Impact of second phase content on rock salt rheological behavior under cyclic mechanical conditions. *Rock Mechanics and Rock Engineering*, **54**: 5245–5267; <https://doi.org/10.1007/s00603-021-02449-4>.
- Mello, U.T., Karner, G.D., Anderson, R.N., 1995.** Role of salt in restraining the maturation of subsalt source rocks. *Marine and Petroleum Geology*, **12**: 697–716; [https://doi.org/10.1016/0264-8172\(95\)93596-V](https://doi.org/10.1016/0264-8172(95)93596-V)
- Mikołajczyk, M., 2008.** Objasnienia do Mapy hydrogeologicznej Polski w skali 1:50 000, arkusz Krośnice (516) – Pierwszy Poziom Wodonośny (in Polish). Państwowy Instytut Geologiczny – PIB, Warszawa.
- Negulic, E., Loudon, K.E., 2017.** The thermal structure of the central Nova Scotia Slope (eastern Canada): seafloor heat flow and thermal maturation models. *Canadian Journal of Earth Sciences*, **54**: 146–162; <https://doi.org/10.1139/cjes-2016-0060>
- Pająk, L., 2005.** Thermal energy exploitation from salt domes. *Proceedings World Geothermal. Congress 2005*, 1145.
- Parecka, K., 1980.** Dokumentacja geologiczna złoża soli kamiennej w wydazie solnym Łanięta, gmina Łanięta, woj. Płock, kat. C1 (in Polish). CAG, Warszawa, nr 13772.
- Peryt, T.M., Kiersnowski, H., 2026.** Perm (in Polish). In: *Budowa geologiczna Polski. Tom 1. Stratygrafia* (ed. T.M. Peryt): 337–402. Państwowy Instytut Geologiczny – PIB, Warszawa; <https://doi.org/10.7306/isbn.9788368623864.pp.337-402>
- Peryt, T.M., Geluk, M.C., Mathiesen, A., Paul, J., Smith, K., 2010.** Zechstein. In: *Petroleum Geological Atlas of the Southern Permian Basin Area* (eds. J.C. Doornenbal and A.G. Stevenson): 123–147. EAGE Publications b.v., Houten.
- Petersen, K., Lerche, I., 1995.** Quantification of thermal anomalies in sediments around salt structures. *Geothermics*, **24**: 253–268; [https://doi.org/10.1016/0375-6505\(94\)00051-D](https://doi.org/10.1016/0375-6505(94)00051-D)
- Piątkowska, A., Surała, M., Perski, Z., Graniczny, M., 2012.** Application of the SAR interferometric methods to identify the mobility of the area above the salt diapir in Inowrocław and the regional salt structures in central Poland. *Geology, Geophysics & Environment*, **38**: 209–220; <https://doi.org/10.7494/geol.2012.38.2.209>
- Poborska-Młynarska, K., 2022.** Geologiczno-górniczne warunki eksploatacji w kopalniach podziemnych w wydazach solnych Polski środkowej (in Polish). Wydaw. Naukowe AGH, Kraków.
- Poborska-Młynarska, K., Burliga, S., Czapowski, G., Misiek, G., Garlicki, A., 2004.** Możliwości utrzymania produkcji w Kopalni Soli „Kłodawa” oraz koncepcje jej likwidacji w świetle obecnego rozpoznania budowy geologicznej, zagrożeń naturalnych i geomechanicznych skutków wieloletniej eksploatacji (in Polish). Etap I. Aktualizacja budowy geologicznej wydazu solnego w granicach obszaru górniczego Kopalni Soli „Kłodawa” z wnioskami dla dalszego jej funkcjonowania Fundacja „Nauka i Tradycje Górnicze”, AGH, Kraków.
- Raymond, J., Langevin, H., Comeau, F.A., Malo, M., 2022.** Temperature dependence of rock salt thermal conductivity: implications for geothermal exploration. *Renewable Energy*, **184**: 26–35; <https://doi.org/10.1016/j.renene.2021.11.080>
- Roman M., 2011.** Objasnienia do Szczegółowej mapy geologicznej Polski w skali 1:50 000, arkusz Gostynin (481) (in Polish). Państwowy Instytut Geologiczny – PIB, Warszawa.
- Sarbu, I., Sebarchievici, C., 2014.** General review of ground-source heat pump systems for heating and cooling of buildings. *Energy and Buildings*, **70**: 441–454; <https://doi.org/10.1016/j.enbuild.2013.11.068>
- Sbrana, A., Marianelli, P., Pasquini, G., Sbrana, M., 2018.** The integration of 3D modeling and simulation to determine the energy potential of low-temperature geothermal systems in the Pisa (Italy) Sedimentary Plain. *Energies*, **11**, 1591; <https://doi.org/10.3390/en11061591>
- Scheck-Wenderoth, M., Cacace, M., Maystrenko, Y.P., Cherubini, Y., Noack, V., Kaiser, B.O., Björn, L., 2014.** Models of heat transport in the Central European Basin System: effective mechanisms at different scales. *Marine and Petroleum Geology*, **55**: 315–331; <https://doi.org/10.1016/j.marpetgeo.2014.03.009>
- Self, J.S., Reddy, V.B., Rosen, A.M., 2013.** Geothermal heat pump systems: status review and comparison with other heating options. *Applied Energy*, **101**: 341–348; <https://doi.org/10.1016/j.apenergy.2012.01.048>
- Sobolewska, A., Żerebiec-Chmielewska, A., Kurkiewicz, M., 2012.** Objasnienia do Mapy hydrogeologicznej Polski w skali 1:50 000, arkusz Gostynin (481) – Pierwszy Poziom Wodonośny (in Polish). Państwowy Instytut Geologiczny – PIB, Warszawa.
- Szewczyk, J., Gientka, D., 2009.** Terrestrial heat flow density in Poland – a new approach. *Geological Quarterly*, **53**: 125–140; <https://doi.org/10.7306/gg.7507>
- Ślizowski, K., Köhsling, J., Lankof, L., 2004.** Uwarunkowania podziemnego składowania odpadów niebezpiecznych w Polsce (in Polish). *Studia, Rozprawy, Monografie*, **129**.
- Tarkowski, R., Bujakowski, W., Uliasz-Misiak, B., 2003.** Powierzchniowe badania geotermiczne nad wydazem solnym „Góra” (in Polish). In: *Termiczna charakterystyka górotworu w rejonie wydazów solnych* (eds. W. Bujakowski and R. Tarkowski): 73–84. IGSMiE PAN, Kraków.
- Teixeira, M.G., Liu, I.S., Rincon, M.A., Cipolatti, R.A., Palermo, L.A., 2014.** The influence of temperature on the formation of salt domes. *International Journal of Modeling and Simulation for Petroleum Industry*, **8**: 35–41.
- Trusheim, F., 1957.** Über Halokinese und ihre Bedeutung für die strukturelle Entwicklung Norddeutschlands. *Zeitschrift der Deutschen Geologischen Gesellschaft*, **109**: 111–151.
- Vizgirda, J., O'Brien, J.J., Lerche, I., 1985.** Thermal anomalies on the flanks of a salt dome. *Geothermics*, **14**: 553–565; [https://doi.org/10.1016/0375-6505\(85\)90006-9](https://doi.org/10.1016/0375-6505(85)90006-9)
- Węgrzyn, A., Nowakowska, M., Sierpiński, D., 2012.** Objasnienia do Mapy hydrogeologicznej Polski w skali 1:50 000, arkusz Lubień Kujawski (480) – Pierwszy Poziom Wodonośny (in Polish). Państwowy Instytut Geologiczny – PIB, Warszawa.

- Włostowski, J., 2002.** Objaśnienia do Mapy hydrogeologicznej Polski w skali 1:50 000, arkusz Kutno (517) – Główny Użytkowy Poziom Wodonośny (in Polish). Państwowy Instytut Geologiczny, Warszawa.
- Włostowski, J., Gregosiewicz, R., 2002a.** Objaśnienia do Mapy hydrogeologicznej Polski w skali 1:50 000, arkusz Gostynin (481) – Główny Użytkowy Poziom Wodonośny (in Polish). Państwowy Instytut Geologiczny, Warszawa.
- Włostowski, J., Gregosiewicz, R., 2002b.** Objaśnienia do Mapy hydrogeologicznej Polski w skali 1:50 000, arkusz Krośnice (516) – Główny Użytkowy Poziom Wodonośny (in Polish). Państwowy Instytut Geologiczny, Warszawa.
- Yu, Z., Lerche, I., Lowrie, A., 1992.** Thermal impact of salt: simulation of thermal anomalies in the Gulf of Mexico. *Pure and Applied Geophysics*, **138**: 181–192; <https://doi.org/10.1007/BF00876399>
- Polish Geological Institute – National Research Institute, n.d. Centralny Bank Danych Hydrogeologicznych – Bank HYDRO. <https://www.pgi.gov.pl/psh/dane-hydrogeologiczne-psh/947-bazy-danych-hydrogeologiczne/9057-bankhydro.html> (accessed December 31, 2025).
- Polish Geological Institute – National Research Institute, n.d. MIDAS – Mineral Resources Data System, map portal. <https://midas-app.pgi.gov.pl/ords/r/public/midas/mapa> (accessed December 31, 2025).